UNIVERSITY *of the*
WESTERN CAPE

The safety and toxicity of MPA-CdTe quantum dots in legume plants.

Zaahira Omar

A mini-thesis submitted in partial fulfilment of the requirements for the degree of

Magister Scientiae in the Department of Biotechnology, University of the Western Cape.

Supervisor: Dr. M Keyster

November 2017

Table of Contents

University of the Western Cape

Private Bag X17, Bellville 7535, South Africa

Telephone: +27-21- 959 2255/959 2762 Fax: +27-21- 959 1268/2266

FACULTY OF NATURAL SCIENCE

Plagiarism Declaration

Name: ……Zaahira Omar……..

Student number: ….3066674……

1. I hereby declare that I know what plagiarism entails, namely to use another's work and to present it as my own without attributing the sources in the correct way. (Refer to University Calendar part 1 for definition)
2. I know that plagiarism is a punishable offence because it constitutes theft.
3. I understand the plagiarism policy of the Faculty of Natural Science of the University of the Western Cape.
4. I know what the consequences will be if I plagiarise in any of the assignments for my course.
5. I declare therefore that all work presented by me for every aspect of my course, will be my own, and where I have made use of another's work, I will attribute the source in the correct way.

---------- 30/11/2017 ----------

Signature Date

Acknowledgements

Firstly, I would like to thank the **Almighty**, without Him none of this would be possible.

I would also like to thank my supervisor **Dr. Marshall Keyster** for all the advice and guidance he has given me with regards to my studies, it was without a doubt invaluable in my success.

My sincerest gratitude to my parents, **Mohamed Mustapha and Shamila Omar and the rest of my family**, for giving me the greatest gift anyone could give another person, complete belief in me. Thank you for your continued support and for always encouraging me to do my best.

A special thanks to **Aalia Essop** for being my version of Schrödinger's cat; there for me even when you weren't. Your support, work ethic and charm kept me sane and motivated.

To **Inshaaf Layloo** and **Aarifah Jakoet**, words cannot express my feelings nor my thanks for all your support.

To the **Environmental Biotechnology Laboratory (EBL) members and fellow lab mates**; thank you for your willingness to lend a helping hand. A special thanks to **Professor Onani** and **Zuraan Paulsen** from the Department of Chemistry for donating their time and lab space.

Lastly, I would like to express my sincerest appreciation to the **University of the Western Cape (UWC), Department of Science and Technology (DST)** and the **National Nanoscience Postgraduate Teaching and Training Platform (NNPTTP)** for giving me the opportunity and means to pursue my goals.

List of Abbreviations

APX	Ascorbate peroxidase
Ca	Calcium
CAT	Catalase
CdTe	Cadmium telluride
Cu	Copper
DNA	Deoxyribonucleic acid
Fe	Iron
FWHM	Full width half maximum
FW	Fresh weight
G. max	*Glycine max*
H_2O_2	Hydrogen peroxide
HR-TEM	High-resolution transmission electron microscopy
ICP-OES	Inductively coupled plasma- optical emission spectrometry
K	Potassium
MDA	Malondialdehyde
Mg	Magnesium
Mn	Manganese
Mo	Molybdenum
MPA	3-mercaptopropionic acid
NP/ NM	Nanoparticle/ Nanomaterial
O_2^-	Superoxide
P	Phosphorus
P. vulgaris	*Phaseolus vulgaris*
PL	Photoluminescence spectroscopy
QDs	Quantum dots
ROS	Reactive oxygen species
SOD	Superoxide dismutase
UV-vis	Ultraviolet-visible spectroscopy
Zn	Zinc

List of Figures

Chapter 1

Chapter 3

Chapter 4

List of Tables

Chapter 4

Supplementary Tables

Keywords

Antioxidant enzymes

Bioimaging

Glycine max

Nanoparticles

Oxidative stress

Phaseolus vulgaris

Quantum dots

Reactive oxygen species

Toxicity

Abstract

The expansion of nanotechnology, resulting in multitudes of consumer and industrial products, causes concern amongst the scientific community regarding the risks associated with the release of nanomaterials into the environment and its subsequent effects on plants. Therefore, the focus of this study was aimed at investigating the effects of MPA-capped CdTe and carbon QDs on legumes plants namely *P. vulgaris* and *G. max*. Fluorescent imaging revealed that QDs were translocated from the roots to the aerial parts of the plant and accumulated in the edible parts of *P. vulgaris*. Subsequent physiological and biochemical tests revealed that both QD types induced oxidative stress as biological markers for stress including lipid peroxidation and cell death were elevated. In addition, carbon QDs displayed lower toxicity in comparison to MPA-CdTe QDs, but still possessed the ability to induce oxidative stress in plant cells. However, the effects were more pronounced in *G. max* in comparison to *P. vulgaris*; and more so with MPA-CdTe QDs than carbon QDs. Furthermore, MPA-CdTe and carbon QDs altered the concentrations and translocation of essential macro and microelements that are required for plant growth and development. This may have detrimental effects on crop productivity and yield, with negative implications on food quality and food security.

Chapter 1

Literature Review

1.1 Introduction

Nanotechnology is the design, fabrication and application of nanostructures or nanomaterials, and the fundamental understanding of the relationships between physical properties and material dimensions (Kroll *et al.,* 2007). It deals with materials or structures typically ranging in size of 0.1 to 100 nm (Nikalje, 2015). On this scale, materials are referred to as nanoparticles (NPs) or nanomaterials (NMs), and may possess new physical properties or exhibit new physical phenomena similar to quantum mechanics, such as changes in the electrical conductance, chemical reactivity, magnetism, optical effects and physical strength in comparison to their bulk counterparts. As a result nanotechnology has become a fast-developing industry, which has a substantial impact on the economy, society and the environment. It has the potential to revolutionize the agricultural and food industry with new tools for molecular disease treatment, rapid disease detection and enhancing a plant's ability to absorb nutrients. Smart sensors and delivery systems will help the agricultural industry fight crop viruses and other pathogens (Santos *et al*., 2010). However, the novel-size dependant properties that make NPs attractive in industry also creates concerns in terms of the environmental and toxicological impact. Thus, the large-scale and unrestricted use of NPs has led researchers to consider the problems, challenges and consequences of their impact (Yang *et al*., 2017). To date, the concentration of NPs in the environment is much lower than the toxic concentration (Batley *et al*., 2013). Thus, the potential health and environmental effects of NPs needs to be thoroughly evaluated before they are widely commercialized in order to prevent NP concentrations in soil from reaching toxic levels. When NPs enter the

soil through agricultural application, atmospheric deposition, rain erosion, surface run-off or other pathways; NPs will accumulate in the soil as a result of their weak migration ability. In addition, exposure modelling indicated that the concentrations of NPs in soil will be higher than those in water or air (Gottschalk *et al*., 2009), implying that soils will most likely be an important sink for NMs that enter the environment. Furthermore, surfactants and other organic acids present in soil can facilitate the mobility of NMs that would have otherwise limited their transport. However, studies relating to the fate and transport behaviour of engineered NMs in solid matrices, such as soil, are very limited (Navarro *et al*., 2011).

As primary producers, plants are vital components for any community to function as they are responsible for converting solar energy into organic matter that can be used by other trophic groups; and are therefore considered fundamental in functional terrestrial ecosystems (Yang *et al*., 2017). As a result plants serve as a potential pathway for the transportation of NPs into ecosystems; through the food chain and can be accumulated in high trophic-level consumers (Zhu *et al*., 2008). The occurrence of oxidative stress is one of the major biochemical alterations following NP exposure, as it disturbs the balance between cellular function and antioxidative defence mechanisms. A number of studies draw particular attention to the vulnerability of animals and plants to NMs (Miralles *et al*., 2012; Husen & Siddiqi, 2014), but the penetration and translocation in plants and the related toxicity mechanisms remains poorly understood. Plant organs are typically protected by coatings and cell walls, nonetheless their sealing capability may be overcome by NPs. Additionally, even though the effects of NP-induced antioxidant changes and their role in the alleviation of phytotoxicity in plant cells have been reported previously, studies regarding the long-term effects of NM exposure to crop plants are limited at present. Given the soaring production of NMs of all

types and the potential for their release into the environment; the subsequent effects on plants and ecosystem health is becoming an increasing concern that needs to be addressed, especially by the appropriate regulatory agencies (Tripathi *et al*., 2017). With this in mind it is also important to consider that with an increasing human population size, the demand for food, feed, and feedstocks for bioenergy and biofactory plants will increase accordingly, and which may be hampered by the already changing climate, water availability, and poor soil quality. Thus, it becomes important to find suitable ways to increase crop productivity and yield with minimal alterations to the environment.

1.2 Nanoagriculture

An emerging and important subdiscipline of nanotechnology, is the field of nanoagriculture, in which NPs are used to increase agricultural productivity by developing suitable nano-growth promoting compounds and nanofertilizers, which is aimed at crop improvement relating to superior plant growth with outstanding yield and nutritional value (Chakravarty *et al*., 2015).

A novel NM-based micronutrient fertilizer could have some important properties, including the targeting of specific soils and the slow release of essential nutrients into the soil, thereby extending the effective duration of nutrient supply of fertilizers (Veronica *et al*., 2005). Nano-sized formulations of mineral micronutrients may improve solubility and dispersion of insoluble nutrients within soil, reduce soil absorption and fixation, and increase bioavailability leading to increased nutrient uptake by plants. Thereby reducing the loss of fertilizer nutrients in the soil through leaching and/or leaking (Montalvo *et al*., 2015; Liu *et al*., 2016). Another major advantage of nanofertilizers is that they may serve as the best micronutrient for plants, whilst simultaneously rejuvenating soil fertility to organic

conditions without any of the detrimental effects caused by conventional chemical fertilizers (Priyanka & Venkatachalam, 2016).

The use of nanofertilizers as micronutrients in agriculture is one of the main strategies for enhancing crop productivity of a nutritionally enriched food supply (Priyanka & Venkatachalam, 2016). The development of low-cost NMs, which are non-toxic to plants, is necessary for the effective use of nanotechnology in agriculture. However, the influence of NMs can vary greatly and depends on the dose, type, shape, structure, duration of exposure, solubility of the NPs used as well as plant species (Mukherjee *et al*., 2016).

1.3 The effect of nanoparticles on plant growth and development

Nanoparticles (NPs) interact with plants which may cause a number of morphological and physiological changes, depending on the properties of NPs. The efficacy of NPs is determined by their chemical composition, size, surface coating, reactivity, and most importantly the dose at which they are effective (Khodakovskaya *et al*., 2012). From their findings, researchers have reported both positive and negative effects of NPs on plant growth and development, and have pointed out that the effect varies from plant to plant (Siddiqui *et al*., 2015).

1.3.1 Seed germination

Plant growth and development starts from the germination of seeds followed by root elongation and shoot emergence; and are considered the earliest signs of growth and development. Therefore, this is an important component required to fully understand the course of plant growth in relation to NPs. Recently, Krishnaraj et al. (2012) studied the effects of biologically synthesized silver NPs (Ag NPs) on hydroponically grown *Bacopa monnieri*'s growth metabolism, and found that biosynthesized Ag NPs resulted in a significant effect on

seed germination by inducing the synthesis of proteins and carbohydrates. Exogenous application of nano-silicon dioxide (nano-SiO_2) and nano-titanium oxide (nano-TiO_2) improved seed germination of soybean by increasing nitrate reductase (Lu *et al*., 2002); and also by enhancing the seeds ability to absorb and utilize water and nutrients in spinach (Zheng *et al*., 2005). In many studies, increasing evidence suggests that zinc oxide NPs (ZnO NPs) increases plant growth and development; Prasad et al. (2012) in peanut; Sedghi et al. (2013) in soybean under drought stress; Ramesh et al. (2014) in wheat and Raskar & Laware (2014) in onion, reported that lower concentrations of ZnO NPs exhibited beneficial effects on seed germination. However, higher doses of ZnO NPs impaired seed germination.

In a separate study by de la Rosa et al. (2013), in which different concentrations of ZnO NPs were applied on cucumber, alfalfa and tomato, and it was found that only the seed germination of cucumber was enhanced. This data suggests that the effect of NPs on seed germination depends on the concentrations of NPs and varies amongst plant genotype.

1.3.2 Plant growth

Raliya & Tarafdar (2013) reported that ZnO NPs induced a significant improvement in *Cyamopsis tetragonoloba*'s plant biomass, shoot and root growth, and root area. It is evident from correlative light and scanning microscopy, and inductive coupled plasma-atomic emission spectrometry that seedling roots of *Vigna radiata* and *Cicer arietinum* absorbed ZnO NPs and promoted the root and shoot length, and root and shoot biomass (Mahajan *et al*., 2011). Bao-shan et al. (2004) reported exogenous application of nano-SiO_2 on *Changbai larch* (*Larix olgensis*) seedlings and found that nano-SiO_2 improved seedling growth and quality, including mean height, root collar diameter, main root length, and the number of lateral roots. Wang et al. (2014) performed an experiment on rice plants treated with quantum dots

(QDs), without QDs and with silica coated QDs, and found that silica coated QDs markedly promoted rice root growth. Additionally, Ag NPs improved plant growth profile (shoot and root length, leaf area) and biochemical attributes (chlorophyll, carbohydrate and protein contents, and antioxidant enzymes) of *Brassica juncea* (*B. juncea*), common bean and corn (Salama 2012; Sharma *et al*., 2012). However, Gruyer et al. (2013) reported that Ag NPs have both positive and negative effects on root elongation depending on the plants species; and observed that root length was increased in barley, but inhibited in lettuce. From this study, it is suggested that the impact of Ag NPs and other NPs on morphology and physiology of plants may be dependent on the size and shape of NPs, and plant genotype (Siddiqui *et al*., 2015).

1.3.3 Photosynthesis

It is apparent that photosynthesis is a key process for plants, as it changes light energy to chemical energy. However, plants can convert only 2-4 % of the available energy in radiation into new plant growth (Kirschbaum, 2011). As a result, scientists are continuously trying to improve this low efficiency conversion by manipulating techniques and genes in plants. From a nanotechnology perspective, many NMs including gold NPs (Au NPs) have been shown to improve the number of leaves, leaf area, plant height, chlorophyll content, and sugar content that has led to better crop yield in *B. juncea* and *Gloriosa superba* (Arora *et a*l., 2012; Gopinath *et al*., 2014). Nano-SiO_2 has been shown to enhance plant growth and development by increasing gas exchange and chlorophyll fluorescence parameters, such as net photosynthetic rate, transpiration rate, stomatal conductance, PSII potential activity, effective and actual photochemical efficiency, electron transport rate and photochemical quench; in *Cucurbita pepo* L. under salt stress (Siddiqui *et al*., 2014) and nano-TiO_2 in

Indocalamus barbatus (Xie *et al*., 2011). In addition, Yang et al. (2006) showed the effects of titanium oxide NPs (TiO_2 NPs) in growing spinach; and reported an increase in light absorbance, hastening of the transport and conversion of light energy, protection of chloroplasts from aging, and prolonging the photosynthetic time of chloroplasts. It was proposed that this is due to TiO_2 NPs protecting chloroplasts from excessive light by augmenting the activity of antioxidant enzymes such as catalase, peroxidase and superoxide dismutase (Hong *et al*., 2005). Qi et al. (2013) also showed improved net photosynthetic rate, conductance to water, and transpiration rate in tomato plants under heat stress with the exogenous application of TiO_2 NPs. According to Lei et al. (2007) nano-anatase strongly promoted whole chain electron transport, photoreduction activity of photosystem II, O_2-evolving and photophosphorylation activity of chlorophyll from spinach chloroplasts, under both visible and ultraviolet light. A number of studies have reported the beneficial effects of NPs on plants, however there is a growing concern with regards to the harmful effects that NPs may present.

1.4 Nanotoxicology in plants

Nanotoxicology is emerging as an important subdiscipline of nanotechnology and involves the study of the interactions of nanostructures with biological systems. It aims to elucidate the relationship between the physical and chemical properties of nanostructures with the induction of toxic biological responses. This information is important in the characterization of NMs in biotechnology, ecosystems, agriculture and biomedical applications (Santos *et al*., 2010).

Nanoparticles such as silver NPs (Ag NPs) are now being widely used commercially due to their antibacterial properties including its ability to induce oxidative stress, which aids in the

toxicity of Ag NPs to bacteria and algae. However, studies by Jiang et al. (2014) and Gopalakrishnan-Nair & Chung (2014) showed that Ag NPs induced oxidative stress in higher plants such as *Spirodela polyrhiza* (*S. polyrhiza*) and *Arabidopsis thaliana* (*A. thaliana*) as shown by a dose-dependent increase in levels of reactive oxygen species (ROS).

1.4.1 Reactive oxygen species (ROS)

ROS are constantly being produced as by-products of a variety of metabolic pathways in a number of cellular components such as mitochondria, chloroplast and peroxisomes. Under normal conditions an equilibrium exists between the production and scavenging of ROS; as molecules that are present in plant cells are scavenged by a variety of antioxidant defence mechanisms (Gill & Tujeta, 2010). However, significant damages occur under stressful conditions and a disturbance in the equilibrium, by various abiotic and biotic factors, results in a rapid increase in the intracellular levels of ROS. The build-up of ROS in plants due to a range of environmental stress factors, is one of the main causes of a reduction in crop yield on a worldwide scale (Gill & Tujeta, 2010). ROS present in plants include:

1.4.1.1 Hydroxyl radicals (OH^-)

Hydroxyl radicals (OH^-) are amidst the most reactive of the ROS molecules, and can be generated from O_2^- and H_2O_2 at ambient temperatures and a neutral pH, in the presence of an appropriate stress (Gill & Tujeta, 2010). A number of studies have reported that TiO_2 NPs generate large amounts of OH^- free radicals thereby leading to DNA damage in animal cell lines (Ghosh *et al*., 2010). However, no relevant reports on OH^- determination in plants induced by NP exposure exists (Yang *et al*., 2017).

Hydroxyl radicals have the potential to react with many biological molecules such as proteins, lipids, DNA and almost all other cellular constituents due to the lack of mechanisms available

to eliminate this form of ROS, and excessive production of OH^- will inevitably result in cell death (Gill & Tujeta, 2010).

1.4.1.2 Superoxide (O_2^-)

About 1-2 % of O_2 consumption in plants leads to the production of superoxide (O_2^-), with the production attributed to the reduction of O_2 during electron transport within chloroplast and other cellular components (Gill & Tujeta, 2010). The toxicity of O_2^- anions is linked to the iron-dependant conversion into highly reactive OH^- radicals (Caro & Puntarulo, 1996).

According to Chen et al. (2014), when wheat seedling roots were exposed to cadmium telluride QDs (CdTe QDs), O_2^- anion generation increased by 330 %, which has the potential to trigger the production of more reactive ROS such as OH^-. This may result in damage to lipids by oxidation and may result in the deterioration of cell structure (Gill & Tujeta, 2010).

1.4.1.3 Hydrogen peroxide (H_2O_2)

The reduction of O_2^- results in the production of hydrogen peroxide (H_2O_2), which is fairly reactive and has a relatively longer half-life of 1 ms when compared to other ROS which have much shorter half-lives of between 2-4 µs (Gill & Tujeta, 2010). The toxicity of H_2O_2 is linked to the iron-dependant conversion into the highly reactive OH^- radicals (Caro & Puntarulo, 1996).

Hydrogen peroxide plays a double role in plants; where at lower concentrations it may act as a signalling molecule which is involved in acclimatisation in response to various abiotic and biotic stresses (Gill & Tujeta, 2010). In wheat plants, treatment with cerium oxide NPs (CeO_2 NPs) triggered the accumulation of H_2O_2 at concentrations which were almost 10 times higher than that of the control (Zhao *et al*., 2012). It was reported by Chen et al. (2014) upon

exposure of wheat seedlings to CdTe QDs for 5 days, it led to the accumulation of H_2O_2 in the roots, as indicated by the 252.94 % increase in the H_2O_2 content in comparison to control plants. At higher concentrations, the excess levels of H_2O_2 in plant cells may inactivate certain enzymes by the oxidation of their thiol-groups (Tewari *et al*., 2006), and inevitably will lead to programmed cell death (Gill & Tujeta, 2010).

1.5 ROS effects on plants

Reactive oxygen species (ROS) such as superoxide, hydrogen peroxide and hydroxyl radicals are extremely reactive and toxic. Under stressful conditions, excessive ROS are produced in plant organelles, where it induces oxidative stress and causes damage to lipids, proteins, carbohydrates and DNA, which inevitably results in cell death (Figure 1) (Gill & Tujeta, 2010).

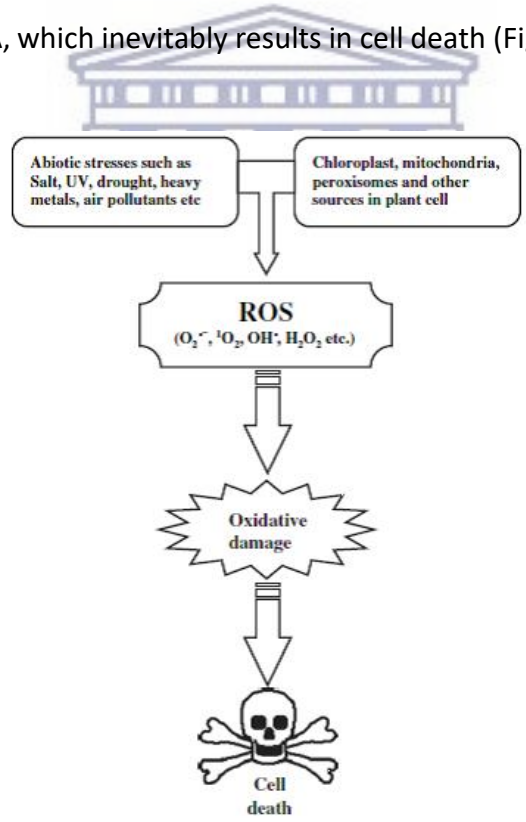

Figure 1: Diagram depicting abiotic stress induced ROS production and cell death. Stresses and organelles which leads to production of ROS, oxidative damage and cell death (Adapted from Gill & Tujeta, 2010).

1.5.1 Lipid peroxidation

The peroxidation of lipids is considered one of the most harmful processes known to living organisms, as it can lead to a decrease in the fluidity of membranes, increased membrane leakage and may cause secondary damage to proteins within membranes (Gill & Tujeta, 2010). Lipid peroxidation is the metabolic process of oxidative deterioration of lipids (Vasilaki & McMillan, 2012) in the membranes of cells and organelles; and occurs when ROS levels reach above threshold and may directly affect normal cellular function (Gill & Tujeta, 2010). It was noted by Cui et al. (2014) when asparagus lettuce (*Lactuca sativa Linn. var. angustata Irish ex Bremer*) was supplemented with varying concentrations of CeO_2 NP suspensions, there was a significant increase in MDA levels after 5 days of treatment. Malondialdehyde (MDA) is a by-product of the peroxidation of unsaturated fatty acids and is indicative of the extent of lipid peroxidation, high concentrations of MDA thus suggests that the production of excess ROS has not been cleared by the plants antioxidant defence systems in a timely manner (Cui *et al*., 2014).

1.5.2 Protein oxidation

Protein oxidation can be defined as the covalent modification of proteins by ROS or by the by-products of oxidative stress. The oxidation of proteins that contain amino acids such as arginine, lysine, histidine, proline, tryptophan and threonine may inhibit, alter their activities and increases their susceptibility to proteolytic attack (Gill & Tujeta, 2010). Protein carbonylation is the most widely used marker and may occur due to the direct oxidation of amino acids in side chains, and ROS are most likely to target proteins that contain amino acids containing sulfur- and thiol-groups. Such reactions can lead to protein damage including enzymes that are involved in DNA repair and synthesis; and the production of aldehyde by-

products such as MDA (Vasilaki and McMillan, 2012). MDA is a highly reactive electrophile that causes toxic stress in cells and interactions with proteins and DNA has often been referred to as being potentially mutagenic and atherogenic; and is widely used as a biomarker to measure the levels of oxidative stress in plants (Del Rio *et al*., 2005). According to Jiang et al. (2014), a significant increase of protein content was found in *S. polyrhiza* after 72 hour exposure to 6 nm Ag NPs at increasing concentrations up to 10 mg/L. Abiotic stresses such as NP exposure can significantly alter protein utilization and protein content in plant tissues as a result of oxidative stress. An increase in protein content in plant tissue, is indicative of Ag NP stress and thus led to the generation of more protein (e.g enzymes) in its detoxification metabolism in order to alleviate stress. However, the highest concentration of 20 nm Ag NPs caused a decrease in protein content in *S. polyrhiza*, indicating that a high concentration of Ag NPs damaged protein generation or accelerated protein decomposition as a result of oxidation, which may inhibit plant growth. The same was noted by Priyanka & Venkatachalam (2016) upon exposure of *Gossypium hirsutum* L. (seedling plants) to ZnO NPs, which resulted in enhanced levels of total soluble protein content, ranging from 126 % to 165.4 % in the treated plants over the control. The increased total soluble protein content correlated positively to the NP dose and it declined slightly following treatment with the highest concentration of 200 mg/L ZnO NPs. These findings further suggest that the up-regulated expression of proteins might protect cells from any oxidative stress caused by NPs.

1.5.3 DNA damage

The most reactive of ROS is OH^- as they have the ability to cause damage to all components of a DNA molecule, by damaging purine and pyrimidine bases and the deoxyribose backbone of the polymer. Singlet oxygen ($^1O_2$) radicals primarily attacks guanine bases, whilst H_2O_2 and

O_2^- do not react. DNA damage due to ROS includes the deletion or modification of a base, cross-linking and strand breakage, as well as the formation of pyrimidine dimers (Gill & Tujeta, 2010). It was noted by Santos et al. (2013) in *Medicago sativa* (*M. sativa*) cells that the number of DNA single and double strand breaks increased with increasing concentrations of 3-mercaptopropionic acid-cadmium selenide/zinc sulphide QDs (MPA-CdSe/ZnS QDs). Enhanced DNA damage (single and double strand breakages detected using a Comet's assay) was thereby linked to oxidative stress. Atha et al. (2012) reported that copper oxide NPs (CuO NPs) induced DNA damage in agricultural and grassland plants; as significant accumulation of oxidatively modified, mutagenic DNA lesions was observed for radish (*Raphanus sativus*), perennial ryegrass (*Lolium perenne*), and annual ryegrass (*Lolium rigidum*) under controlled laboratory conditions. Similarly, damages to the chromosome and micronuclei of *Allium cepa* was observed; and DNA shearing and fragmentation was also found, therein causing the reduction in root growth upon treatment with TiO_2 NPs (Ghosh *et al*., 2010).

1.5.4 Damage to photosynthetic machinery

Chlorosis can be defined as the abnormal yellowing of plant tissues as a result of the partial failure in the development of chlorophyll. When plants undergo stress, there is an increase level of ROS in many organelles including the chloroplast; ROS accumulation leads to photo-inhibition, photo-oxidative damage and eventually cell death (Tsurushima *et al*., 2010). It was observed by Chen et al. (2014), that treatment of wheat seedlings with CdTe QDs resulted in a reduction of chlorophyll *a* and *b* concentrations by 83.96 % and 90.82 % respectively in comparison to control plants. The same study showed a reduction of total chlorophyll concentration by 86.12 % after 5 days of exposure. Qian et al. (2013) reported a potential mechanism of phytotoxicity is that Ag NPs adsorbed via the root surface, which

disrupted the structure of the thylakoid membrane and decreased chlorophyll content, herein causing an inhibitory effect on plant growth.

In order to prevent excessive damage in plant cells under oxidative stress, plants utilize a range of non-enzymatic and enzymatic defence systems to scavenge or reduce ROS within cells (Sharma *et al*., 2012).

1.6 ROS scavenging antioxidant enzymes

1.6.1 Catalase (CAT)

Catalase (CAT) is one of the indispensable enzymes for ROS detoxification when plants are under stressful conditions. It is a heme-containing enzyme with a tetrameric structure, which has the ability to potentially dismutate H_2O_2 into H_2O and O_2. One molecule of CAT has the ability to convert approximately 6 million H_2O_2 molecules into H_2O and O_2 per minute and has one of the highest turnover rates (Gill & Tujeta, 2010). According to Riahi-Madvar et al. (2012) treatment of *Triticum aestivum* (*T. aestivum*) plants with 200 mg/L of alumina NPs (Al NPs) resulted in an increased CAT activity, followed by a decrease in activity with increasing NP concentrations. A study by Samadi et al. (2015) showed a significant increase in CAT activity with treatment of *Melissa officinalis* L. with 100, 200 and 300 mg/L of TiO_2 NPs. An increase in CAT activity, which is responsible for scavenging H_2O_2, may result in reduced production of O_2^- anions preventing lipid peroxidation and further production of OH^- radicals following the uptake of NPs.

1.6.2 Superoxide dismutase (SOD)

It was reported by Li et al. (2009) that *Brassica campestris* cultivars under copper stress showed a significant increase in superoxide dismutase (SOD) activity. SOD is a metalloenzyme

which is classified by their metal cofactors (Cu/Zn, Mn and Fe) and is known as the most effective antioxidant enzyme (Gill & Tujeta, 2010). This enzyme forms the first line of defence against the effects of toxic levels of ROS, and is responsible for the removal of O_2^- by catalysing the dismutation; one O_2^- being reduced to H_2O_2 and the other oxidized to O_2 (Gill & Tujeta, 2010). According Jiang et al. (2014), treatment of *S. polyrhiza* with varying concentrations of Ag NPs (0.5-10 mg/L) resulted in a significant increase in SOD activity in comparison to the control, and the results suggested that the activity was dose dependent. A study by Riahi-Madvar et al. (2012) showed that treatment of *T. aestivum* plants with 200 and 500 mg/L of Al NPs resulted in a 121.43 % and 135.71 % increase in SOD activity, respectively, whereas treatment with 1000 mg/L resulted in a decrease in SOD activity. The up-regulation of SOD to a certain point, followed by a down-regulation under stressful conditions is highly expected in order to combat oxidative stress.

1.6.3 Ascorbate peroxidase (APX)

During different stress conditions plants have demonstrated an enhanced expression of ascorbate peroxidase (APX); which is involved in scavenging H_2O_2 with high affinity in water-water and ascorbate-glutathione (ASH-GSH) cycles, where ASH is used as the electron donor (Gill & Tujeta, 2010). However, a study by Riahi-Madvar et al. (2012) showed APX activity is significantly decreased in the presence of Al NPs in *T. aestivum*, except for 200 mg/L treatment which was similar to the control plants. Similarly, Chen et al. (2014) demonstrated the effect of CdTe and CdTe with the additive effect of UV-B radiation in the roots of wheat seedlings. The toxicity was manifested by decreased levels of antioxidant enzymes including APX, and the more pronounced effects in the roots is presumably due to the release of additional Cd^{2+} as a result of surface oxidation of QDs under UV-B radiation.

1.7 Quantum dots (QDs)

Quantum dots (QDs) are inorganic semiconductor nanocrystals comprised of groups II–VI or III–V elements, whose excitons (excited electron-hole pairs) are confined in all three dimensions, giving rise to unique and characteristic fluorescent, optical, electrical, photochemical and photophysical properties. QDs are extremely photostable, bright and are characterized by broad absorption profiles, high extinction coefficients, and narrow and spectrally tuneable emission profiles (Santos *et al*., 2010). QDs are being increasingly used in industrial and biological applications, and the incorporation of QDs into commercial products would indicate a potential for their release into different environmental compartments, from point and diffuse sources, e.g. manufacturing waste, intentional release in applications, disposal of consumer products and medical waste (Navarro *et al*., 2011). This may result in a considerable amount of QDs being released into the ecosystem, raising an equal amount of concern due to the possible toxic effects in living organisms, particularly crop plants (Chen *et al*., 2014). Thus, numerous studies have suggested capping toxic and hydrophobic QDs with hydrophilic molecules such as dihydrolipoic acid (DHLA) and mercaptopropionic acid (MPA) in order to render them biocompatible and water soluble (Figure 2). However, those same properties that make them biocompatible, may also facilitate their uptake by biological systems (Yu *et al*., 2012; Santos *et al*., 2013).

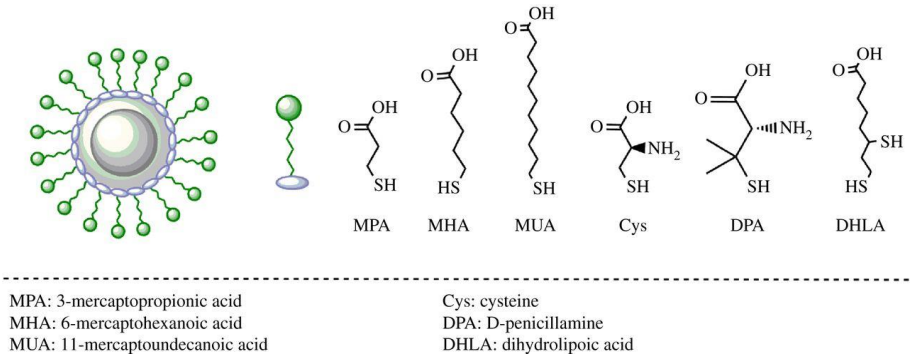

Figure 2: Diagram depicting small molecule ligands with affinity towards the surface of quantum dots. Small molecular weight thiolated ligands are used to impart hydrophilicity and biocompatibility. The thiol-groups on these ligands bind to the surface of quantum dots and the terminal carboxylic acid or amine functional groups (Adapted from Banerjee *et al*., 2016).

Cadmium telluride and cadmium selenide QDs, typically encased in zinc sulphide shells (CdTe and CdSe QDs) are the most frequently used QDs. However, the toxicity of CdTe and CdSe QDs is of increasing concern due to their small size (2-10 nm) and heavy metal formulation (Chen *et al*., 2012; Chen *et al*., 2014). According to Yu et al. (2014), the cytotoxicity of CdTe QDs was shown to be associated with their concentration and the duration of exposure, as the results demonstrated that treatment with QDs enhanced the production of ROS in *Arabidopsis* stem cells, and the relative concentration of ROS increased over time with continuous treatment. CdTe QDs release free cadmium ions (Cd^{2+}) under UV-B radiation, leading to the disruption of DNA replication, the generation of ROS and subsequently oxidative stress. This effect is likely to be further exacerbated by the increasing levels of solar UV radiation at the Earth's surface due to the depletion of stratospheric ozone (Chen *et al*., 2014). Furthermore, the toxicity of CdTe QDs has been shown to be much higher than that of Cd^{2+} and that the cytotoxicity was not solely due to free Cd^{2+} (Cho *et al*., 2007). In addition, cellular toxicity was found to be closely related to the size of QDs, with smaller diameter QDs (2 nm) demonstrating more toxic effects than larger QDs (5 nm) (Lovrić *et al*., 2005). Hoshino

et al. (2004) also reported that surface modification of QDs changes their physicochemical properties and that the cytotoxicity of QDs was dependent on their surface molecules (Figure 2).

Due to the inherent toxic state of CdTe QDs as a result of their heavy metal formulation, there is an increased interest in cadmium and heavy metal-free QDs such as carbon QDs. Carbon QDs are carbon-based NPs and are constituted by an intrinsically non-toxic element, which makes them useful and promising as bio-analytical tools (Wang & Hu, 2014). Carbon is commonly known as a black material, and is considered to have low solubility in water and weak fluorescence. Yet, at the nanoscale, carbon has high solubility and strong fluorescence. Carbon QDs are small in size and offers unique properties including high photostability and quantum yield, strong fluorescence and fluorescent lifetime, biocompatibility and chemical inertness; and these properties can be exploited in various applications including bio-imaging, bio-sensing, drug delivery etc. Thus, carbon QDs offer the same outstanding features as heavy metal-containing QDs, however the advantage of carbon QDs is the low toxicity, environmental friendliness and ease of synthesis on a large-scale at lower costs, as it can be produced from agricultural solid wastes such as sugarcane bagasse, coir, pineapple and banana leaves etc. (Thambiraj & Shankaran, 2016; Namdari *et al*., 2017).

1.8 Conclusion

The receptivity and response of plants to NPs goes beyond the predictable ones, as it has become evident that the effect of NPs varies from plant to plant and depends on their mode of application, size, concentration and type of NP. Within cells, NPs may interact with molecules directly and indirectly through mechanisms still poorly understood. As a result, the level of highly reactive molecular species of oxygen (ROS) is likely to increase, with the

potential to damage any biomolecule including lipids, proteins and DNA; and even activate programmed cell death mechanisms. The typical cellular response is an increase of antioxidant enzymes; so the changes in the cellular rate of ROS and anti-ROS and peroxidation products allow us to assess the degree of toxicity of NPs and the detoxifying ability of plant cells. Oxidative stress induced by NPs may have long-term effects in some plant cells and in the case of the up-regulation of certain genes it can benefit plant growth and thus should be considered as potentially exploitable as nanofertilizers in agriculture. As an extension it becomes our responsibility and a priority to weigh up the potential benefits of NPs for plants and humans against the risk of exposing terrestrial ecosystems to NPs.

1.9 Justification

Engineered nanoparticles (NPs) are widely used in cosmetics, electronics, optical devices, medicine, agriculture, etc. The unique properties of these materials may present adverse effects to both organisms and the environment. Plants as the basic components of the ecosystem are easily exposed to NPs in atmospheric, terrestrial and aquatic environments. Moreover, NPs that enter into plants may be transferred to herbivorous consumers and further cause potential negative effects to the health of human beings. Accordingly, the interactions between NPs and plants are of particular concern (Miralles *et al*., 2012; Cui *et al*., 2014).

However, in plants, uptake, accumulation and internalization of NPs does not readily indicate an immediate toxic effect. In addition, plants have various physical defence structures and chemical defences that allow them to adapt to different types of environmental stressors, which displays discrepancies between cultivar and species (Zhu *et al*., 2008; Santos *et al*., 2010). A number of toxicity studies have been conducted both *in vitro* and *in vivo* over the

past decade (Kong *et al*., 2011), however due to the lack of standardized preparation protocols, coatings, doses, and application systems of NPs, the observed toxic effects are inconsistent. Therefore, it is imperative that studies to examine the effects of NMs are conducted in a variety of plant systems in order to build suitable databases with regards to safety and toxicity. Thus, the focus of the present study was to investigate the potential toxicity and safety of MPA-capped CdTe and carbon QDs in legumes, *Phaseolus vulgaris* (*P. vulgaris*) and *Glycine max* (*G. max*).

1.10 Aims and objectives

- Synthesize water-soluble MPA-CdTe QDs.
- Characterise MPA-CdTe and carbon QDs using UV-vis and PL spectroscopy, and HR-TEM.
- Visualise the uptake and translocation of QDs in *P. vulgaris* and *G. max* using *in vivo* fluorescent bioimaging.
- Assess the physiological effects after QD exposure including plant biomass, lipid peroxidation, cell death and chlorophyll content.
- Determine the levels of reactive oxygen species (ROS) including O_2^- and H_2O_2.
- Quantify the levels of ROS scavenging enzymes such as SOD, CAT and APX.
- Assess the macro and micro nutrient profiles of *P. vulgaris* and *G. max* using ICP-OES.

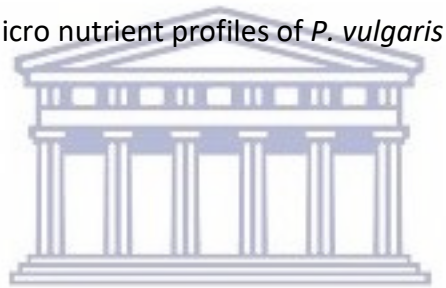

1.11 Highlights

- Water-soluble MPA-CdTe QDs were successfully synthesized.
- MPA-CdTe and carbon QDs were successfully characterized using HR-TEM, PL and UV-vis spectroscopy.
- MPA-CdTe and carbon QDs were subsequently imaged *in vivo* in *P. vulgaris* and *G. max* showing uptake from the soil and translocation from the roots to the leaves.
- Images generated by the IVIS Lumina imaging system revealed translocation and accumulation in the bean pods of *P. vulgaris*.
- MPA-CdTe and carbon QDs initiated oxidative stress in *P. vulgaris* and *G. max*.
- Carbon QDs displayed lower toxicity in comparison to MPA-CdTe QDs, but still possessed the ability to induce oxidative stress in plant cells.
- A number of macro and microelement concentrations in the roots of *P. vulgaris* and *G. max* increased, yet the overall translocation between roots, shoots and leaves decreased.

Chapter 2

Materials and Methods

2.1 Synthesis of MPA-capped CdTe quantum dots

3-Mercaptopropionic acid capped-cadmium telluride quantum dots (MPA-CdTe QDs) were synthesized according to previous studies with some modifications (Chomoucka *et al*., 2013; Yan *et al*., 2010). The first step of synthesis involved the preparation of NaHTe solution through the reduction of 0.04 mmol tellurium (Te) with 1 mmol sodium borohydride ($NaBH_4$) in deionized water. This solution was subsequently heated to 80 °C for 30 minutes. A second solution was prepared containing 0.4 mmol cadmium chloride ($CdCl_2$) and 0.6 mmol 3-mercaptopropionic acid (MPA) dissolved in 15 ml of deionized water (pH 11.7), this solution was heated to 100 °C under inert atmospheric conditions forming the Cd/MPA precursor. However, prior to reaching the final temperature, the NaHTe solution was injected at 80 °C and the reaction was then maintained at 100 °C for 2 hours to allow for CdTe nanocrystal growth. Thereafter, the solution was degassed and heated to 90 °C for 1 hour which allowed the growth of MPA-capped CdTe QDs. The solution was then cooled and centrifuged to remove unreactive material, and the resultant QD solution was stored in the absence of light for subsequent analysis. Carbon QDs was purchased from Sigma Aldrich (http://www.sigmaaldrich.com – SKU: 900414).

2.2 Characterization of MPA-capped CdTe and carbon quantum dots

Initial analysis of both MPA-capped CdTe and carbon QDs was performed using ultraviolet-visible (UV-vis) absorption and photoluminescence (PL) spectroscopy. UV-vis absorption spectra was measured at room temperature using Nicolet Evolution 100 (Thermo Scientific)

and PL emission spectra using Nanolog (HORIBA, Jobin Yvon). Data was then represented as graphs using OriginPro 2017 software. Subsequently, high resolution-transmission electron microscopy (HR-TEM) studies were performed using the Hitachi H800, operated at 200 kV. MPA-CdTe and carbon QDs size and distribution was determined manually using ImageJ software.

2.3 Plant growth and treatment parameters

P. vulgaris and *G. max* seeds were imbibed in sterile deionized water for 1 hour, and then sown in pots containing a soil: filtered silica sand with a ratio of 1:3, respectively. The treatments commenced once plants had grown to the V2 stage (when the second trifoliolate leaves are fully expanded), which involved applying 300 µM MPA-CdTe and carbon QD solutions to the respective plant directly onto the soil, consecutively for a period of 5 days. The same parameters were applied to control plants with the exception of deionized water as the treatment.

To determine plant biomass, the leaves and roots were placed in an oven at 65 °C for 48 hours in order to obtain the dry weight. The remaining leaf and root material was snap-frozen in liquid nitrogen, ground into a fine powder and stored at - 80 °C for further analysis.

2.4 *In vivo* imaging of MPA-CdTe and carbon QDs within *P. vulgaris* and *G. max*

Bioimaging of QDs within fresh plant structures was performed using the IVIS® Lumina II Imaging System and Living Image software version 3.0 (Caliper Life Science). For MPA-CdTe QDs, two filter sets were used, namely: GFP filter set which included an emission filter (515-575 nm), excitation filter (445-490 nm) and a background filter (410-440 nm) and Cy 5.5 filter set which included an emission filter (695-770 nm), excitation filter (615-665 nm) and a background filter (580-610 nm). Similarly, for carbon QDs the GFP filter set was used which

included an emission filter (515-575 nm), excitation filter (445-490 nm) and a background filter (410-440 nm). Subsequently, the resultant images were overlayed using the system software. The image acquisition was performed using the following system parameters: subject height 0.5 cm, field of view 12.5 cm, lamp level high and an automatic exposure time (0.5-60 seconds).

2.5 Assessment of oxidative damage

2.5.1 Lipid peroxidation by quantifying MDA levels

A modified method by Zhang et al. (2007) was used to determine MDA levels: 100 mg of frozen plant material from each sample was weighed out, homogenized in 6 % trichloroacetic acid (TCA) and centrifuged at 14 000 rpm for 30 minutes. A volume of 200 µl of the supernatant was incubated with 20 % TCA/0.5 % 2-thiobarbituric acid (TBA) solution at 95 °C for 20 minutes. This was followed by incubation on ice for 10 minutes and centrifugation at 14 000 rpm for 5 minutes. The absorbance of the supernatant mixture was read at 532 nm and corrected for non-specific absorbance at 600 nm. Subsequently, the MDA content was determined using the extinction coefficient, ε = 155 μM^{-1} cm^{-1} and expressed as nmol. g^{-1} fresh weight (FW).

2.5.2 Estimation of cell death

The extent of cell death was determined by means of a spectrophotometric assay aimed at measuring the amount of Evans blue retained by non-viable cells (Sanevas *et al*., 2007). For measurement in the leaves, 1 cm^3 blocks were cut from the leaf edge and from the roots, 2 cm fragments were cut from the root tip. The material was then placed into Eppendorf tubes containing 1 ml of 0.25 % Evans blue and incubated at room temperature for 1 hour. The unbound dye was washed off, and the leaf and root material incubated in deionized water

overnight at room temperature. The water was subsequently discarded and the material placed in 1 % (w/v) aqueous sodium dodecyl sulfate (SDS) and incubated at 65 °C to release the trapped Evans blue from the cells. Subsequently, the absorbance of the supernatant was measured spectrophotometrically at 600 nm.

2.5.3 Chlorophyll *a* and *b* content

A modified method by Sumanta et al. (2014) was followed to determine chlorophyll content: 100 mg of frozen leaf material was added to foil wrapped Eppendorf tubes in order to prevent the degradation of chlorophyll *a* and *b*, ten volumes of 100 % (v/v) acetone was then added to the same Eppendorf tube and vortexed briefly. Once mixed, the samples were then analysed spectrophotometrically in 1 ml quartz cuvettes in triplicate at 662 nm and 644 nm, respectively.

2.6 Assays for ROS determination

2.6.1 Spectrophotometric assay for determination of hydrogen peroxide content

A modified method by Velikova et al. (2000) was used to determine H_2O_2 content as described below: 100 mg of frozen plant material from each sample was weighed out, homogenized in 6 % TCA and centrifuged at 14 000 rpm for 30 minutes. A volume of 50 µl of the supernatant was added to separate wells of a microtitre plate (in triplicate) along with 5 mM dipotassium phosphate (K_2HPO_4) buffer (pH 5) and 0.5 M potassium iodide (KI). A standard was also prepared using 0.5 M KI, 5 mM K_2HPO_4 buffer and 0.1 mM H_2O_2. The absorbance of the reaction mixture was measured at 390 nm, and H_2O_2 content was determined using the extinction coefficient, ε = 0.28 μM^{-1} cm^{-1} and expressed as mmol. g^{-1} FW.

2.6.2 Spectrophotometric assay for determination of superoxide content

The determination of O_2^- was performed as previously described by Russo et al. (2015) with amendments. For measurement in the leaves, 1 cm^3 blocks were cut from the leaf edge and from the roots, 2 cm fragments were cut from the root tip for each treatment and placed into an Eppendorf tube containing 1 ml of a reaction mixture containing: 10 mM H_2O_2, 10 mM potassium cyanide (KCN), 80 µM nitrotrezolium blue choride (NBT), 2 % SDS and 50 mM phosphate buffer (KPO_4); and incubated at room temperature for 20 minutes. Subsequently, the plant material was crushed and pelleted by centrifugation at 13 000 rpm for 5 minutes. The samples were then analyzed spectrophotometrically at 560 nm and the O_2^- levels calculated using the extinction coefficient, ε = 12.8 mM^{-1} cm^{-1} and expressed as µmol. g^{-1} FW.

2.7 Assays for antioxidant enzymes

2.7.1 Protein extraction and quantification

Protein extraction on leaf and root samples was performed as previously describe by dos Santos Soares et al. (2010) with modifications: 100 mg of frozen material was weighed out into three separate Eppendorf tubes (three tubes per plant sample). A volume of 500 µl protein extraction buffer containing; 4 mM phosphate buffer, 1 mM ethylenediaminetetraacetic acid (EDTA) and 5 % (w/v) polyvinylpyrrolidone (PvP) was then added to one of the three tubes and vortexed. After the mixture had been adequately mixed, the plant material was then pelleted by centrifugation at 12 000 rpm for 5 minutes. The supernatant was then removed and introduced into the second tube of the respective sample. The previous steps were then repeated for the second and third tube. After the last centrifugation step, the supernatant from the third tube was removed and inserted into a

clean Eppendorf tube. The protein concentrations were then quantified using a Bradford assay, and the samples were stored at - 20 °C until subsequent analysis.

2.7.2 A kinetic spectrophotometric assay to determine superoxide dismutase activity

The superoxide dismutase (SOD) activity was determined using a modified method by Garcia-Limones et al. (2002). A volume of 10 µl of each protein extract was loaded onto a microtitre plate containing 20 mM phosphate buffer, 0.1 mM NBT, 0.005 mM riboflavin, 10 mM methionine and 0.1 mM EDTA, and incubated for 20 minutes on a light box at room temperature. Following incubation the samples were analysed spectrophotometrically at 560 nm and the activity was calculated and expressed as SOD units. mg^{-1} FW.

2.7.3 A kinetic spectrophotometric assay to determine catalase activity

The catalase (CAT) activity was determined using a modified method of Barka (2001). The principle of the assay is hinged on a decrease in absorbance as a result of the dissociation of H_2O_2 by catalase. A volume of 10 µl protein extract was added to 500 µl reaction mixture containing 100 mM K_2HPO_4 (pH 7.0), 0.5 mM EDTA and 1 mM H_2O_2. The absorbance was read spectrophotometrically at 240 nm in quartz cuvettes in triplicate and the activity was determined using the extinction coefficient, Ɛ = 39.4 mM^{-1} cm^{-1} and expressed as nmol. min^{-1} mg^{-1}.

2.7.4 A kinetic spectrophotometric assay to determine ascorbate peroxidase activity

The ascorbate peroxidase (APX) activity was determined using a modified method by dos Santos Soares et al. (2010). A volume of 20 µl of protein extract was aliquoted into Eppendorf tubes containing 2 mM ascorbate and incubated for 5 minutes. After incubation, a volume of 10 µl of each protein sample was loaded in triplicate into a microtitre plate containing 71.43

mM K_2HPO_4 and 0.36 mM ascorbate. In order to start the reaction, 0.714 mM H_2O_2 was added and the reaction was then measured spectrophotometrically at 290 nm and the activity was calculated using the extinction coefficient, Ɛ = 2.8 mM^{-1} cm^{-1} and expressed as nmol. min^{-1} mg^{-1}.

2.8 Quantification of macro and micro nutrients in plant tissue by ICP-OES

A modified method by Havlin & Soltanpour (2006) was used for the quantification of macro and micronutrients in the leaves and roots of *P. vulgaris* and *G. max*; in which 200 mg of frozen plant material was digested in 1.5 ml of 62 % nitric acid (HNO_3) for 1 hour at 75 °C. Following digestion, each sample was diluted (1:10, v/v) in 2 % HNO_3. The samples were then analysed by axially-viewed inductively coupled plasma optical emission spectrometry (ICP-OES, Varian Inc.).

Chapter 3

Characterisation and *in vivo* imaging of quantum dots to trace uptake and translocation in *P. vulgaris* and *G. max*

3.1 Abstract

Nanoparticles (NPs) have found their applications in a diverse number of fields, including therapy, diagnostics and targeted delivery; thus the visualization of NPs can be exceedingly useful in the tracking of targeted drug and nutrient delivery systems. For this reason, highly luminescent CdTe and carbon QD NPs were used for imaging the uptake and transport of QDs to various plant structures in *P. vulgaris* and *G. max*. The study revealed that the pattern of accumulation and distribution differed between *P. vulgaris* and *G. max* for both MPA-CdTe and carbon QDs, and it appears that uptake and translocation was NP-dependent. Additionally, intact QDs accumulated in the pods of *P. vulgaris*, thus providing evidence of potential trophic transfer for QDs.

3.2 Introduction

It has been made evident that manufactured or engineered nanoparticles (NPs) are capable of reaching different components of the environment including fresh water, air, soil, etc. either through their handling or accidently through modes such as landfills, sewage sludge and wastewater during their synthesis (Gottschalk *et al*., 2009; Prasad *et al*., 2016); with soils acting as the final sink or major contaminant sources of NPs (Cornelis *et al*., 2014). Possible uptake and accumulation of NPs in plants, especially in the edible parts, has raised great concern over human exposure from food web contamination. However, very few studies have explored the possibility of NP transfer from plant uptake into a potential food web and

there remains a critical gap in knowledge regarding trophic level transfer of NPs through food chains that are more closely relevant to human consumption (Koo *et al*., 2015). Furthermore, the underlying mechanisms of NP uptake and translocation by plants remains poorly understood. NPs and NP-containing solutions are dynamic; they possess the ability to aggregate and dissolve under various conditions. In addition, plants can take up various ions from the growth medium or soil and reductively precipitate them as particles (Gardea-Torresdey *et al*., 2003; Beattie & Haverkamp, 2011). Therefore, the presence of particles in a plant is not always definitive proof of the plant's ability to take up and translocate intact NPs. For that reason, QDs are particularly well-suited for studying intact NP uptake in plants. QDs are not only useful for tracking particle uptake and movement within a variety of organisms, but fluorescence will only be detected when intact core-QDs are present, as the breakdown components are very unlikely to reconstitute into fluorescent QDs within plants, providing evidence that intact NPs were taken up by the plant (Mancini *et al*., 2008; Koo *et al*., 2015). In addition, QDs appear to be a useful platform for *in vivo* fluorescence monitoring in plants, as a result of their tuneable size characteristics, as their emission spectra can be shifted towards regions with minor autofluorescence. This is useful as it represents a special challenge for fluorescence imaging in plants due to autofluorescent molecules inherently present in plant leaves and stems (Vaneckova *et al*., 2016). Thus, the aim of the present study was to investigate the uptake and translocation of MPA-CdTe and carbon QDs within *P. vulgaris* and *G. max* using the IVIS Lumina Imaging System.

3.3 Results

3.3.1 Characterisation of MPA-CdTe and carbon QDs

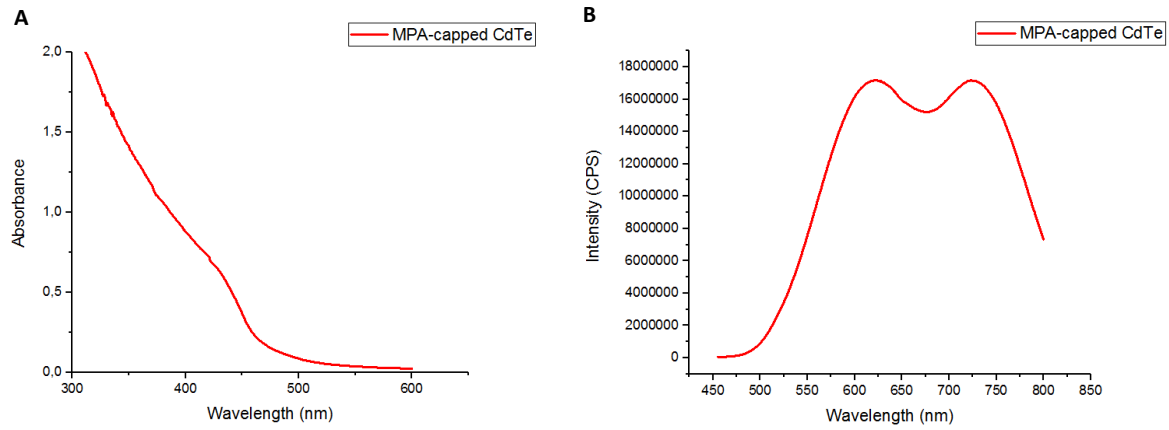

Figure 1: UV-vis & PL characterisation of MPA-CdTe QDs. A) UV-vis absorption spectra of MPA-CdTe QDs with excitation wavelength of 440 nm B) Photoluminescent spectra of MPA-CdTe QDs with emission wavelength between 550 nm and 750 nm.

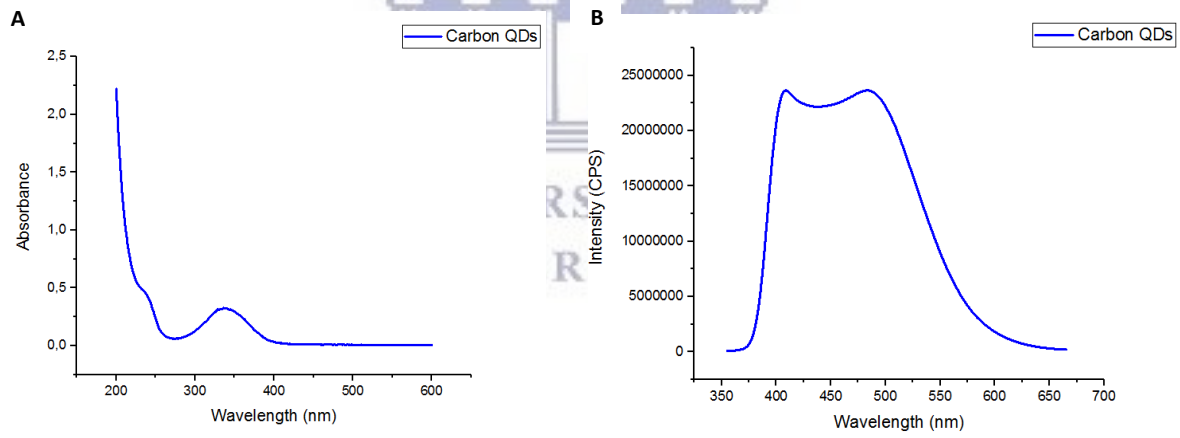

Figure 2: UV-vis & PL characterisation of carbon QDs. A) UV-vis absorption spectra of carbon QDs with excitation wavelength of 340 nm B) Photoluminescent spectra of QDs with emission wavelength between 400 nm and 550 nm.

The initial characterization of water-soluble MPA-CdTe and carbon QDs nanoparticles was performed using UV-Vis absorption and photoluminescence spectroscopy. The UV-vis absorption spectrum of MPA-CdTe QDs revealed an absorption peak at 440 nm (Figure 1A) and PL spectrum revealed a full width half maximum (FWHM) of 242 nm and a wide emission

spectra from 550-750 nm with emission peaks at 622 nm and 726 nm (Figure 1B). The UV-vis absorption spectrum of carbon QDs shown in Figure 2A reveals a typical absorption peak observed at 220 nm, which is attributed to the π- π* transition for aromatic sp^2 hybridisation for carbon QDs (Thambiraj & Shankaran, 2016) and a peak at 340 nm. The carbon QDs PL spectrum revealed FWHM of 149 nm and exhibited a wide emission spectra from 400-550 nm with emission peaks at 407 nm and 484 nm (Figure 2B).

Subsequent analysis of QDs was accomplished using HR-TEM (Figure 3A & 4A). The resulting images displayed relatively monodispersed MPA-CdTe and carbon QD NPs, with some showing a tendency to aggregate. Additionally, the images revealed particles which are spherical in shape with average diameters ranging from 5-6.5 nm and 3.5-4.5 nm, which correlates to the characteristic orange-red and yellow colour emitting QDs, for MPA-CdTe and carbon QDs, respectively (Figure 3B & 4B).

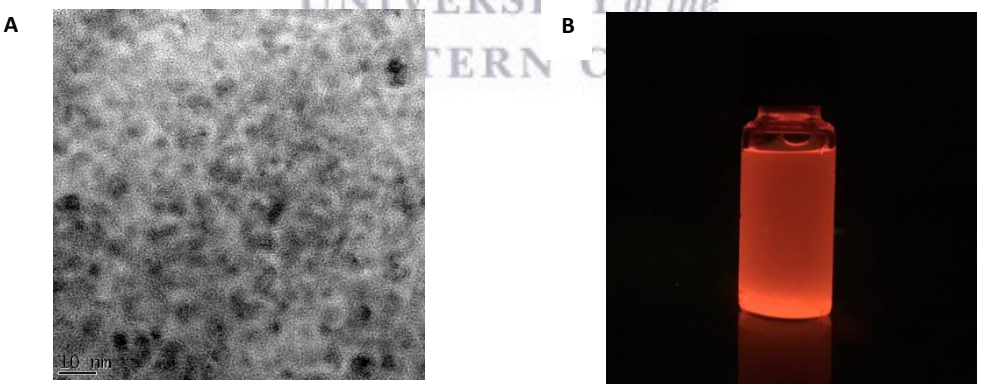

Figure 3: HR-TEM characterisation of MPA-CdTe QDs. A) HR-TEM micrograph B) under UV-light.

According to Peng and co-workers (Peng et al., 2003; Li et al., 2013), extinction coefficient (**ε**) of MPA-CdTe QDs can be determined by the following equation:

$$\varepsilon = 10043(D)^{2.12}$$

Wherein **D** (nm) is the diameter or size of a given nanocrystals sample and **ε** is the extinction coefficient of the corresponding sample.

The diameter (**D**) of the MPA-CdTe QDs was determined as 5 nm using HR-TEM and ImageJ software, and the extinction coefficient (**ε**) was calculated as 3.05×10^5 L. mol^{-1} cm^{-1} according to the aforementioned equation. Subsequently, the concentration of the MPA-CdTe QDs was determined as 1.87×10^{-6} M using Beer-Lambert's law. Carbon QDs concentration was provided by manufacturer at 0.2 % (2 mg/ml).

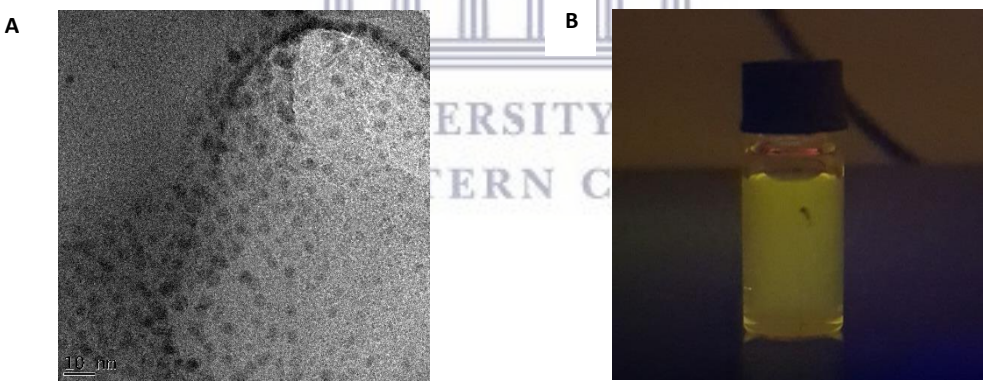

Figure 4: HR-TEM characterisation of carbon QDs. A) HR-TEM micrograph B) under UV-light.

3.3.2 *In vivo* imaging of MPA-CdTe and carbon QDs within *P. vulgaris* and *G. max*

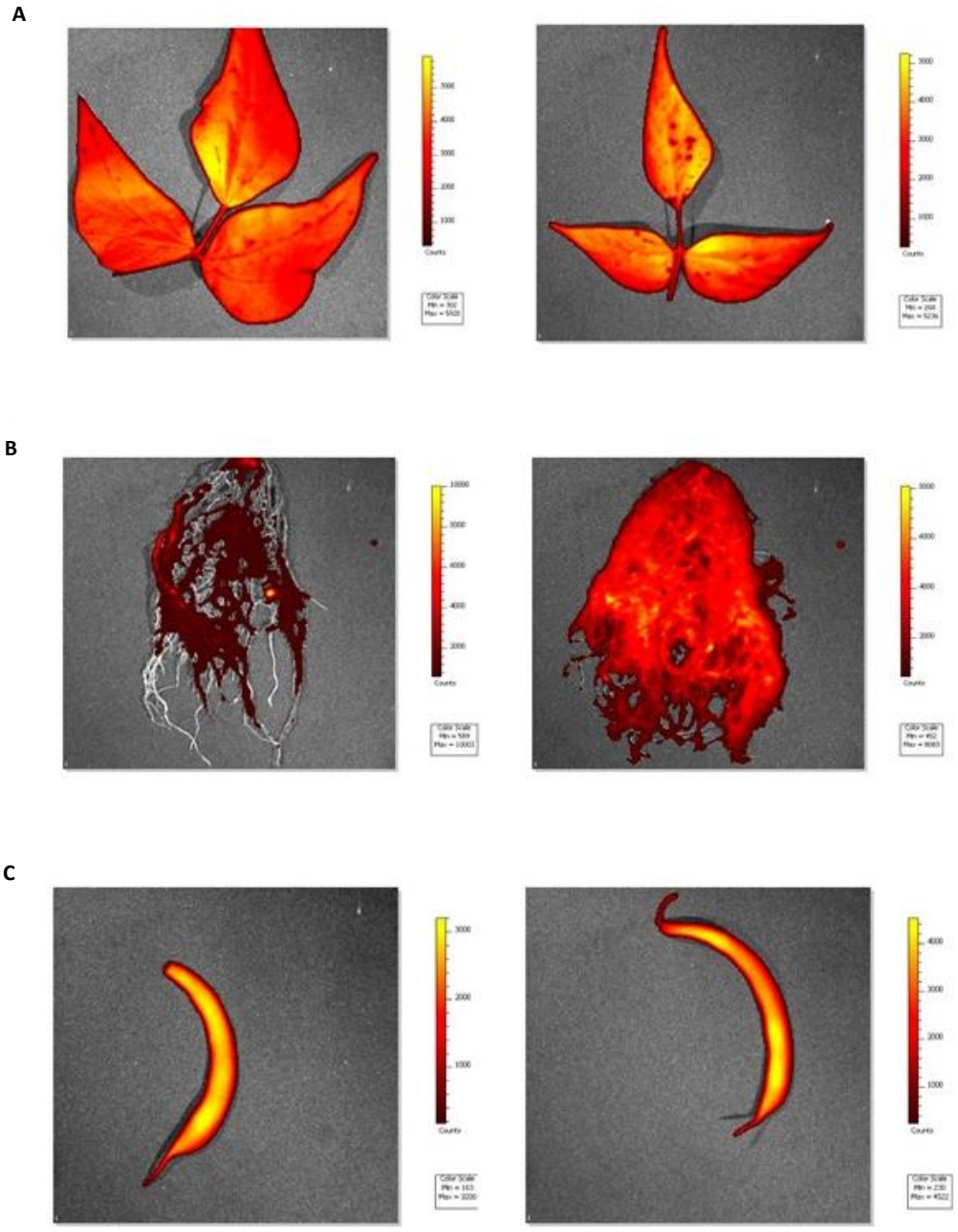

Figure 5: *In vivo* fluorescent images of MPA-CdTe QDs within *P. vulgaris*. Control (left) and MPA-CdTe QDs (right). A) Whole leaf fluorescence image B) Whole root fluorescence image and C) Whole pod fluorescence image. Colour bars indicate the relative intensity of light emitted. Each image is a representative of a set of 9 images.

A series of *in vivo* experiments were performed in order to evaluate the potential use of QDs in assessing NP uptake and transport in plants. Two NP modifications have been examined namely MPA-CdTe and carbon QDs in both *P. vulgaris* and *G. max*. Treatment of *P. vulgaris* and *G. max* with MPA-CdTe and carbons QDs revealed uptake in the roots and subsequent translocation to the leaves as can be seen by the relative increase in fluorescent intensity as indicated by a more intense and widespread yellow colour, in comparison to the respective controls (Figure 5 & Figure 6).

The uptake of MPA-CdTe QDs in *P. vulgaris* suggests a widespread distribution within the roots as can be seen by the change in colour from a deep red to a bright read indicating greater fluorescence, with some translocation to the leaves and pods (Figure 5). Similarly, in carbon QD-treated *P. vulgaris* plants, uptake is evident with greater translocation to the leaves as indicated by the more widespread yellow colour than in the control (Figure 6). This difference in the intensity of light suggests that *P. vulgaris* retains a larger portion of MPA-CdTe particles within the roots (Figure 5B right) and carbon QDs in the leaves (Figure 6A right). However, in both MPA-CdTe and carbon QD-treated plants a similar distribution pattern can been seen in the leaves, with the QDs emitting light from the periphery of the leaves (Figure 5A & 6A right). Furthermore, for both treatments translocation to the bean pods can be seen, however the accumulation was greater as seen by a greater maximum intensity in the MPA-CdTe QD-treated *P. vulgaris* plants in comparison to carbon QD-treated plants (Figure 5C & 6C).

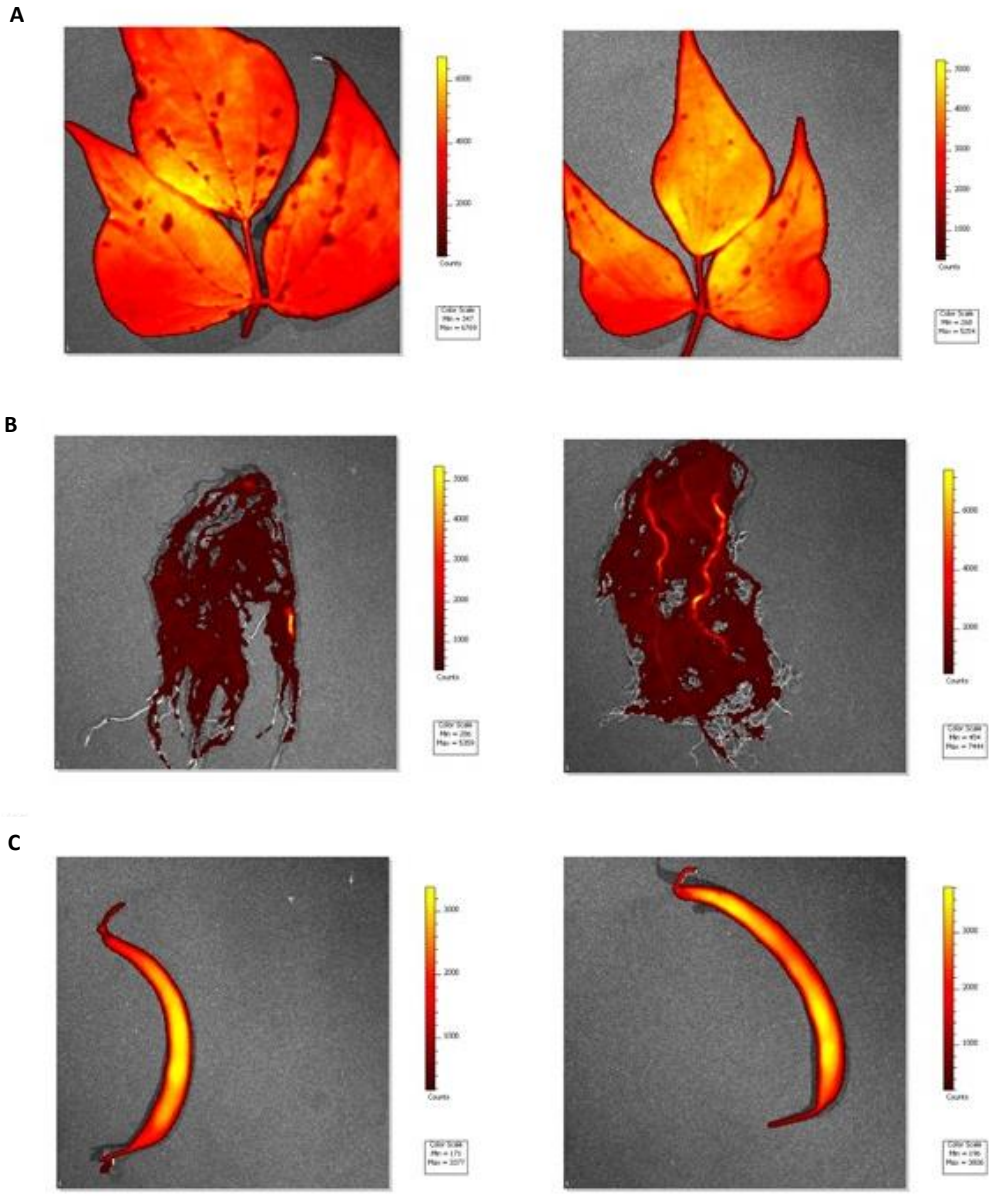

Figure 6: *In vivo* fluorescent images of carbon QDs within *P. vulgaris*. Control (left) and carbon QDs (right). A) Whole leaf fluorescence image B) Whole root fluorescence image and C) Whole pod fluorescence image. Colour bars indicate the relative intensity of light emitted. Each image is a representative of a set of 9 images.

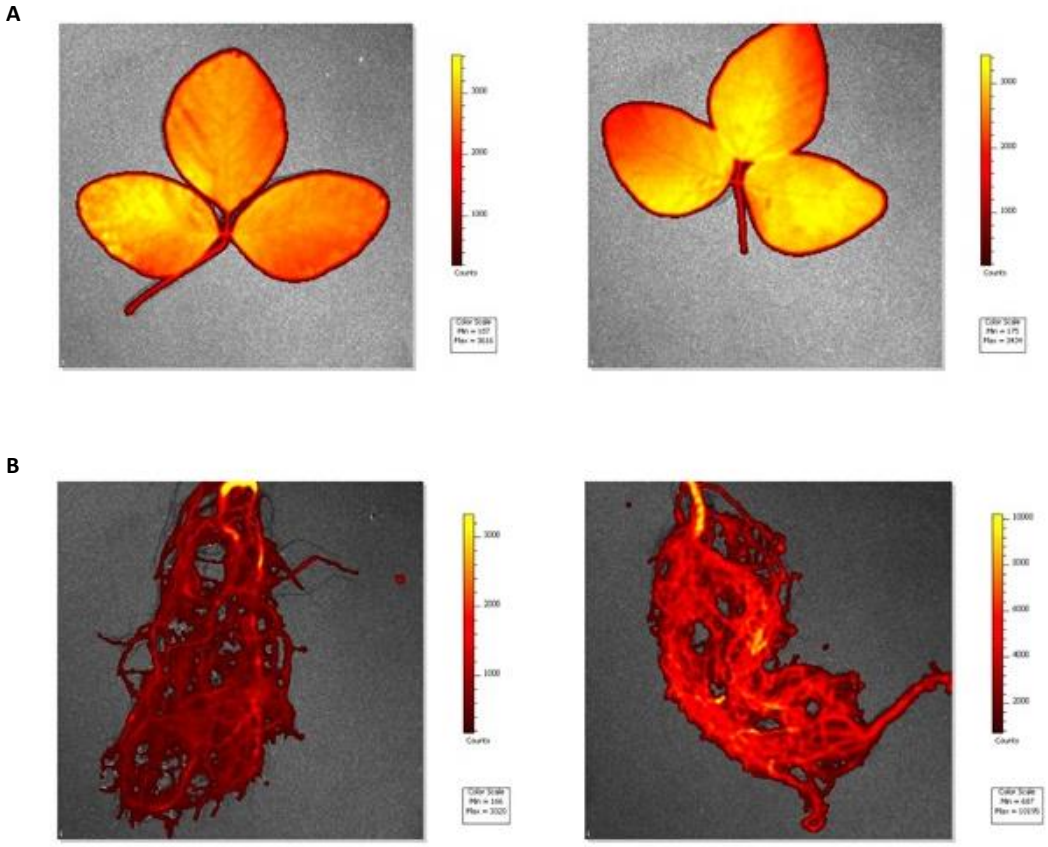

Figure 7: *In vivo* fluorescent images of MPA-CdTe QDs within *G. max*. Control (left) and MPA-CdTe QDs (right). A) Whole leaf fluorescence image B) Whole root fluorescence image. Colour bars indicate the relative intensity of light emitted. Each image is a representative of a set of 9 images.

In vivo imaging of MPA-CdTe QD-treated *G. max* plants revealed translocation to the leaves with maximum retention of the NPs within the roots as indicated by a higher overall fluorescence as indicated by a change from deep red to a bright red in comparison the control and higher maximum relative intensity (Figure 7B right). A similar trend was observed for carbon-QD treated plants as a higher relative intensity was observed in the roots in comparison to the leaves, suggesting that *G. max* retains a larger proportion of QD NPs within the roots (Figure 8). In addition, in both MPA-CdTe and carbon QD-treated plants a similar distribution pattern can been seen in the leaves, with the QDs emitting fluorescent light from

the centre of the leaves, which indicates that QDs tend to accumulate in the central part of the leaf and then spread outward (Figure 7A & 8A right).

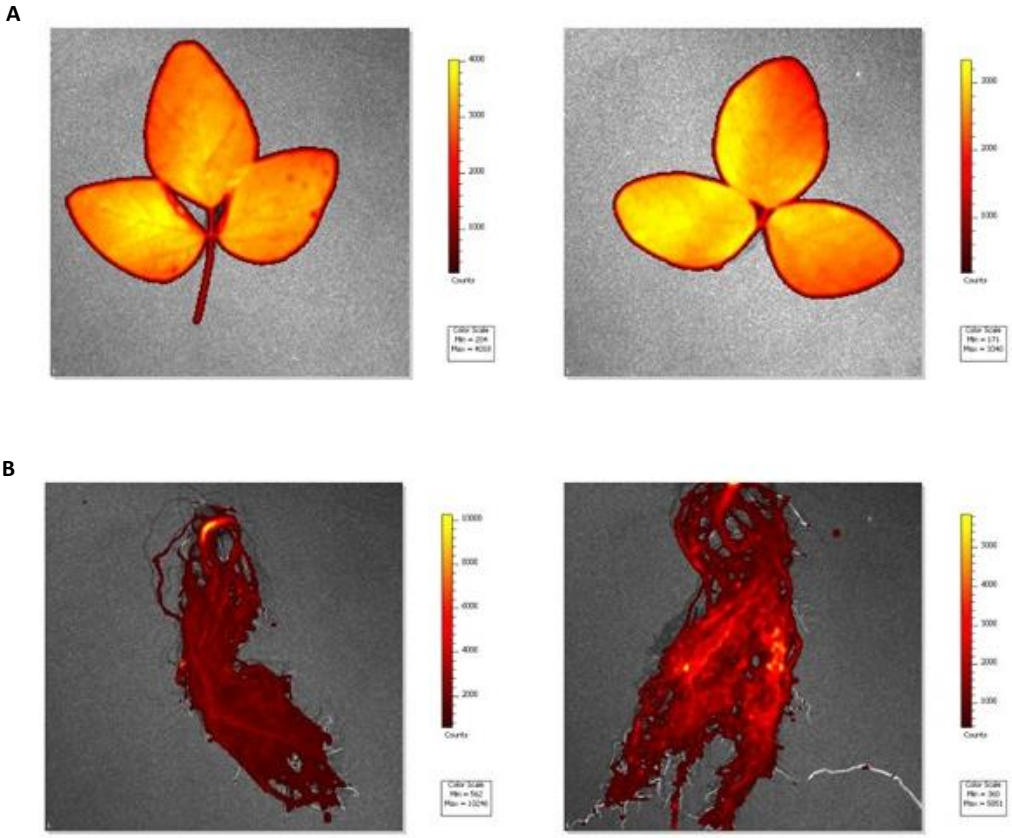

Figure 8: *In vivo* fluorescent images of carbon QDs within *G. max*. Control (left) and carbon QDs (right). A) Whole leaf fluorescence image B) Whole root fluorescence image. Colour bars indicate the relative intensity of light emitted. Each image is a representative of a set of 9 images.

3.4 Discussion

The initial characterisation of both MPA-CdTe and carbon QDs was performed by UV-vis absorption and photoluminescence spectroscopy. The excitation wavelength for MPA-CdTe and carbon QDs obtained from UV–vis absorption spectra was 440 nm and 340 nm, respectively. In addition, the UV-vis spectrum of carbon QDs (Figure 2A) yielded two characteristic peaks, one at 220 nm corresponding to π-π* transition of the conjugated C=C

band and another at 280 nm corresponding to n-π* transition of C=O band (Shereema *et al*., 2015). The subsequent emission spectrum displayed PL peaks at 662 nm and 726 nm for MPA-CdTe QDs, and 407 nm and 484 nm for carbon QDs. These findings are in agreement with those by Frasco & Chaniotakis (2009), who reported emission wavelengths between 500-700 nm for orange-emitting Cd QDs and Li et al. (2016) who reported emission wavelengths between 400-600 nm for yellow-emitting carbon QDs. Moreover, Duan et al. (2009) and Singh et al. (2013) reported that broad FWHM of PL curves can be attributed to a wide size distribution of QDs; analysis using HR-TEM confirmed fairly monodispersed, spherical MPA-CdTe and carbon QDs, with some showing a tendency to aggregate and a relatively wide size distribution, which correlates to the broad FWHM of 242 nm and 149 nm observed for MPA-CdTe and carbon QDs, respectively. In a separate study by Shen et al. (2013), it was suggested that a broad size distribution and a small surface/volume ratio significantly decreases the quantum yield. However, it is important to note that the QDs synthesized and used in this study was sufficient for use in the assessment of uptake, translocation and accumulation in *P. vulgaris* and *G. max*.

Several studies have been proposed concerning plant uptake of NPs and their examination in plants. *In vivo* fluorescent bioimaging systems represents great potential for the examination and monitoring of NPs within plant structures. In plants, autofluorescence of biomolecules such as chlorophyll, carotene and xanthophylls, represents a critical problem in fluorescence imaging (Vaneckova *et al*., 2016). However, by using adequate excitation and emission filters during image acquisition, this phenomenon can be effectively suppressed. In a study by Koo et al. (2015), *A. thaliana* plants that were exposed to poly acrylic acid-ethylene glycol QDs (PAA-EG QDs) emitted clear fluorescence of varying intensity from nearly all leaves, thus providing evidence of uptake and translocation of intact QDs from the roots to

the aerial leaves. In the present study, it is evident that both *P. vulgaris* and *G. max* absorbed intact MPA-CdTe and carbon QDs from the soil, with MPA facilitating the uptake of CdTe QDs (Yu *et al*., 2012; Santos *et al*., 2013); and transporting it from the roots to the leaves. A clear difference can be seen between control and QD-treated plants as fluorescence is only detected when intact core-QDs are present, as the breakdown components are not likely to reconstitute into fluorescent QDs inside of the plant (Mancini *et al*., 2008; Koo *et al*., 2015). However, the pattern of accumulation differed between the plant and QD type. For *P. vulgaris*, MPA-CdTe QDs accumulated at higher levels in the roots than leaves, whereas carbon QDs accumulated at higher levels in the leaves than roots. Contrastingly, *G. max* accumulated higher levels in the roots for both MPA-CdTe and carbon QDs. Furthermore, the pattern of distribution in the leaves were plant species dependant rather than QD dependant. Additionally, both MPA-CdTe and carbon QDs have accumulated in the bean pods of *P. vulgaris*, yet the extent of accumulation was greater for MPA-CdTe QDs. A study by Kote et al. (2013) reported similar findings of translocation of fullerenes to the flowers and fruit of bitter melon plants as well as an increase in fruit yield. However, the translocation and accumulation of certain NPs; specifically heavy-metal containing NPs such as CdTe QDs used in the present study; into edible parts of a plant raises a number of concerns regarding food web contamination, specifically food chains closely related to human consumption.

Many physiochemical variations exist amongst plant species, such as differences in hydraulic conductivity, cell wall pore size, etc. as well as molecule/ion uptake and translocation kinetics, which may influence the transport and accumulation of NPs in various plant structures (Tripathi *et al*., 2017). It is proposed that NPs penetrate the cell wall and cell membrane of root epidermis and accompanied by a complex series of events, enters the plant's vascular bundle, and then moves to the stele, to be translocated to the leaves, with

xylem serving as the most important vehicle in the distribution and translocation of NPs. A study by Wang et al. (2012) in *Zea mays* L. treated with CuO NPs demonstrated uptake and distribution from root to shoot through xylem and the reverse through phloem. In sunflower, tomato and pea plantlets treated with magnetic carbon-coated NPs; ranging from 5 to 50 nm; the NPs were absorbed by the roots and then translocated to the xylem vessels up to the leaves, with a different efficiency depending on the plant species and NP size (Cifuentes *et al*., 2010). The unique optical properties of the carbon dots allowed the authors to visualize their transport by means of apoplastic paths from the roots to the stems and leaves by the vascular system in mung bean plants (Li *et al*., 2016). Similarly, corn plants treated with CeO_2 NPs, penetrated the roots and translocated in the shoots along a path that seemed to be apoplastic (Zhao *et al*., 2012). Liu et al. (2009) found that labelled single-walled carbon nanotubes (SWCNTs) were able to cross cell walls and the cell membrane through endocytosis in *Catharanthus* plants and Onelli et al. (2008) observed both clathrin-independent and clathrin-dependent pathways in *Nicotiana tabaccum* for the internalization of Au NPs.

It appears that uptake, translocation and accumulation is NP and plant dependent (Zhang *et al*., 2015). In addition, a number of studies have pointed out that organic substances within the soil influences the mobility of NPs, and that alginates favour NP accumulation in the roots and translocation to shoots (Zhao *et al*., 2012; Zhao *et al*., 2014). However, once NPs have been taken up and accumulation occurs within plant structures, it becomes imperative to investigate and assess the physiological and biochemical effects that may occur after QD exposure.

Chapter 4

Physiological and biochemical effects of quantum dots on *P. vulgaris and G. max*

4.1 Abstract

Nanotechnology is a fast-developing industry, having substantial impact on the economy, society and the environment. The increased use of NPs may have detrimental effects on the environment, especially on crop plants, as more NPs and NP-related pollutants are leached into the soil. Consequently, it becomes necessary to understand how plants respond to NP-induced oxidative stress. It is evident from this study that MPA-CdTe and carbon QDs induced oxidative stress in *P. vulgaris* and *G. max* as indicated by increased MDA content, cell death, ROS and the activation of antioxidant enzyme systems. Furthermore, MPA-CdTe and carbon QDs altered the concentrations and affected the translocation of essential macro and microelements that are required for plant growth and development.

4.2 Introduction

Nanotechnology is an emerging field of science endowed with far ranging applications in cancer therapy, biomedicines, waste water treatment, cosmetics, electronics and agriculture (Nel *et al*., 2006). In recent years, different types of NMs have become more attractive in agronanotechnology due to their promising effects on crop plants. NMs are easily absorbed, similar to organic molecules and inorganic ions from nutrient solutions, inducing various physiochemical changes such as the growth and development of plants and biomass etc. Nevertheless, the influence of NMs can vary greatly and is dependent on the dose, type, shape, structure, duration of exposure and solubility of the NPs used (Mukherjee *et al*., 2016).

The development of low-cost NMs which are not toxic to plants is highly essential for the effective use of nanotechnology in agriculture. Nanoagriculture is mainly aimed at crop improvement relating to superior plant growth with high yield. Yet, numerous studies have reported NPs as the cause of toxicity at certain concentrations affecting productivity of crops by altering their physiological, biochemical and genetic constitutions (Tripathi *et al*., 2016). Biochemical changes mainly result in the generation of excess reactive oxygen species (ROS) including H_2O_2, OH^-, and O_2^- free radicals, which consequently results in oxidative stress, lipid peroxidation, protein and DNA damage in plants. However, plants inherently possess defence strategies in order to overcome the toxicity caused by stressful conditions such as NPs; including various enzymatic and non-enzymatic defence systems. Enhanced levels of antioxidative enzymes, such as superoxide dismutase (SOD), catalase (CAT), and ascorbate peroxidase (APX), have been shown to assist plants in alleviating oxidative stress induced by NPs. However, beyond a limit of stress factors, the internal detoxification mechanisms may fail to overcome the toxicity and this ultimately leads to apoptosis in plant cells (Shen *et al*., 2010). As plants absorb NPs, translocate them to the shoots and it accumulates in various aerial parts of the plant, the possibility of their cycling in the ecosystem increases through the various trophic levels. After accumulation, they start degrading the quality of crops by lowering the germination rate of seeds, decreasing the fresh and dry biomass and the length of roots and shoots of plants, and altering the process of photosynthesis (Tripathi *et al*., 2017). However, studies regarding the long-term physiological and biochemical effects of NP exposure on crop plants are limited at present. Hence, the present study aimed at assessing the possible phytotoxic effects of MPA-CdTe and carbon QDs on *P. vulgaris* and *G. max* by examining plant growth and biomass, chlorophyll content, lipid peroxidation, ROS production, antioxidant enzyme activities and nutrient content.

4.3 Results

4.3.1 Plant growth and biomass

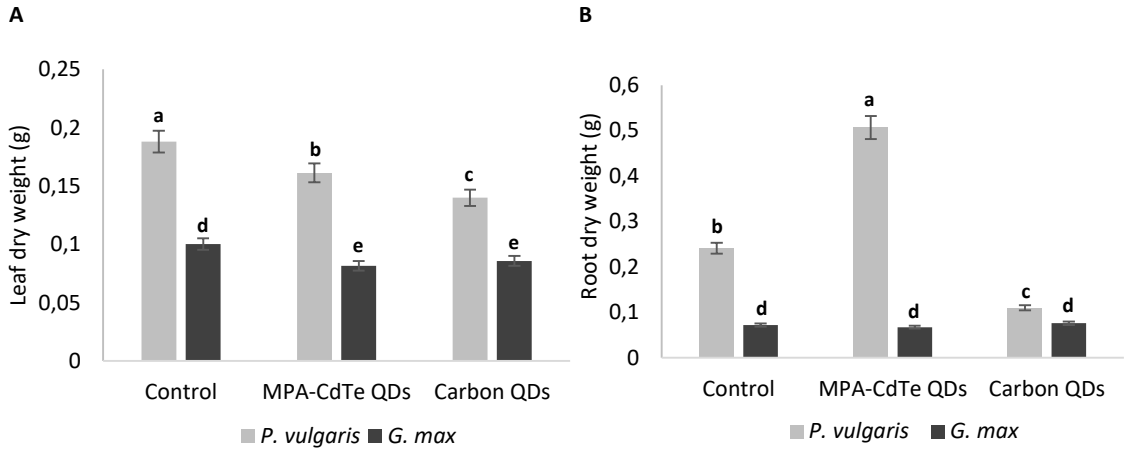

Figure 1: Effect of MPA-CdTe and carbon QDs on plant biomass in *P. vulgaris* and *G. max*: A) Displays the effect on leaf biomass B) Displays the effect on root biomass. Data represents the mean ±SD (n = 3). Means with the same letter are not significantly different ($p < 0.05$).

In order to assess the effects of MPA-CdTe and carbon QDs on plant growth in *P. vulgaris* and *G. max*, the leaf and root dry biomass was compared. For *P. vulgaris*, a 14.25 % and 25.55 % decrease in leaf biomass was observed for MPA-CdTe and carbon QDs when compared to control plants. Furthermore, a 54.22 % decrease in biomass was observed for carbon QDs in the roots. Interestingly, for MPA-CdTe QDs a significant increase in dry biomass by 110.5 % was observed in the roots of *P. vulgaris*. A reduction of 18.51 % and 14.37 % was observed in the leaves of *G. max* for MPA-CdTe and carbon QDs in comparison to control plants. Additionally, a 6.52 % decrease and 5.48 % increase in root biomass was observed for MPA-CdTe and carbon QDs, respectively (Figure 1A & B).

4.3.2 Lipid peroxidation

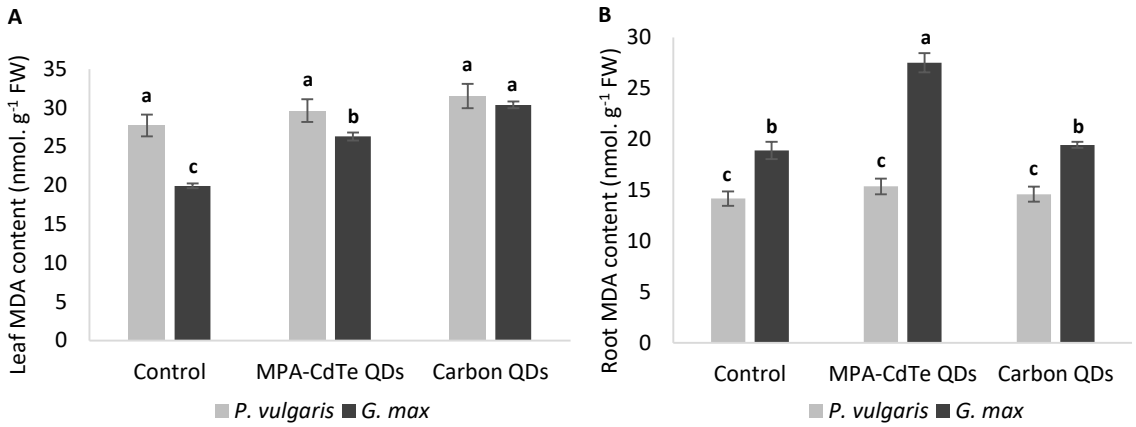

Figure 2: Effect of MPA-CdTe and carbon QDs on lipid peroxidation as indicated by MDA content in *P. vulgaris* and *G. max*: A) Displays the effect on leaf MDA content B) Displays the effect on root MDA content. Data represents the mean ±SD (n = 3). Means with the same letter are not significantly different ($p < 0.05$).

A study by Cabiscol et al. (2010) reported that NPs can affect lipid peroxidation through the generation of ROS, and this significantly affects the fluidity and permeability of membranes and consequently the acquisition kinetics of nutrients. Therefore, the extent of lipid peroxidation was assessed in *P. vulgaris* and *G. max* by measuring the MDA content; which is a by-product of lipid peroxidation. In the leaves of *P. vulgaris*, the MDA content was higher in plants treated with carbon QDs than MPA-CdTe QDs, 6.92 % and 13.71 % respectively in comparison to the control. For *G. max*, the overall increase in MDA content was greater than that of *P. vulgaris*, with 31.99 % and 52.41 % for MPA-CdTe and carbon QDs, respectively (Figure 2A). In the roots, *G. max* exhibited the largest increase of 45.53 % in MDA content for MPA-CdTe QDs and 2.84 % increase for carbon QDs. In *P. vulgaris*, the MDA content increased by 8.39 % and 2.98 % compared to control plants for MPA-CdTe and carbon QDs, respectively.

4.3.3 Cell death

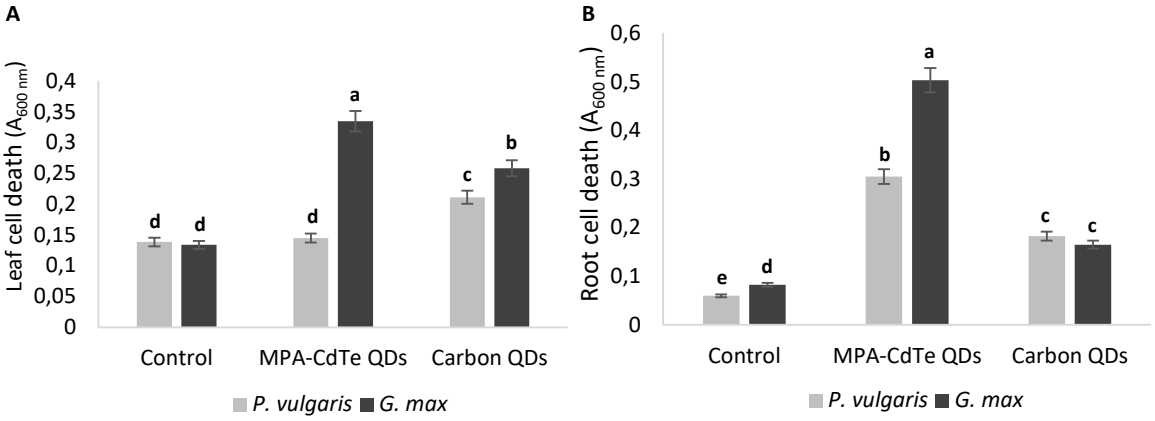

Figure 3: Effect of MPA-CdTe and carbon QDs on plant cell viability in *P. vulgaris* and *G. max*: A) Displays the effect on leaf cell viability B) Displays the effect on root cell viability. Data represents the mean ±SD (n = 3). Means with the same letter are not significantly different ($p < 0.05$).

A number of studies have demonstrated that NPs cause phytotoxicity through the production of ROS which results in oxidative stress, and subsequently leads to necrosis and apoptosis (cell death) (Nair *et al*., 2010). In order to assess cell death after treatment with MPA-CdTe and carbon QDs in *P. vulgaris* and *G. max*, an Evans blue assay was performed on the leaves and roots. Upon treatment with MPA-CdTe and carbon QDs, *P. vulgaris* and *G. max* experienced a loss in both leaf and root cell viability (Figure 3A & B). In the leaves, *P. vulgaris* experienced the highest cell death of 52.53 % increase in comparison to the control upon treatment with carbon QDs, followed by an increase in 4.58 % upon treatment with MPA-CdTe QDs. Contrastingly, *G. max* experienced the highest cell death for MPA-CdTe QDs in the leaves with an increase of 150.13 % in comparison to the control, and a 93.03 % increase for carbon QDs (Figure 3A). In the roots, *G. max* experienced the highest cell death with a 528.75 % increase, followed by *P. vulgaris* with an increase in 407.66 % in comparison to the control plant for treatment with MPA-CdTe QDs. Moreover, in the roots of plants treated with

carbon QDs, *P. vulgaris* experienced a higher cell death compared to *G. max* with an increase in 203.88 % and 106.25 %, respectively (Figure 3B).

4.3.4 Chlorophyll content

Numerous studies have reported that plants treated with NPs experience chlorosis (a loss of green colour in their leaves), as a result of either a decreased chlorophyll production or the alteration of chlorophyll content (Ma *et al*., 2013). As a result, the chlorophyll content in *P. vulgaris* and *G. max* was measured after treatment with MPA-CdTe and carbon QDs. In *P. vulgaris*, MPA-CdTe QDs decreased chlorophyll *a*, *b* and total chlorophyll content by 19.8 %, 34.1 % and 30.31 %, respectively. Whereas, upon treatment with carbon QDs chlorophyll *a*, *b* and total chlorophyll content increased by 14.65 %, 47.61 % and 9.43 % in comparison to the control (Table 1). Similarly, in *G. max* MPA-CdTe QDs decreased chlorophyll *a*, *b* and total chlorophyll content by 17.71 %, 4.66 % and 8.15 %, respectively. Whereas, chlorophyll *a*, *b* and total chlorophyll content increased by 1.89 %, 21.29 % and 16.08 % in comparison to the control upon treatment with carbon QDs (Table 2).

Table 1: Effect of MPA-CdTe and carbon QDs on chlorophyll *a* and *b* content (mg. g^{-1}) in *P. vulgaris.*

	Chlorophyll a	Chlorophyll b	Total chlorophyll
Control	46.41 ± 0.51 [a]	128.7 ± 1.15 [a]	175.11 ± 2.04 [a]
MPA-CdTe QDs	37.22 ± 0.17 [b]	84.81 ± 0.59 [b]	122.02 ± 0.53 [b]
Carbon QDs	53.21 ± 0.18 [c]	138.5 ± 0.56 [c]	191.71 ± 0.91 [c]

Different letters indicate significant difference between means at P < 0.05 (DMRT) per column. Values are means ± SD (n=3).

Table 2: Effect of MPA-CdTe and carbon QDs on chlorophyll *a* and *b* content (mg. g^{-1}) in *G. max*.

	Chlorophyll a	Chlorophyll b	Total chlorophyll
Control	41.79 ± 1.28 [a]	114.53 ± 1.33 [a]	156.33 ± 2.21 [a]
MPA-CdTe QDs	34.39 ± 0.16 [b]	109.19 ± 0.74 [b]	143.58 ± 1.11 [b]
Carbon QDs	42.58 ± 0.94 [a]	138.89 ± 3.51 [c]	181.47 ± 2.45 [c]

Different letters indicate significant difference between means at P < 0.05 (DMRT) per column. Values are means ± SD (n=3).

4.3.5 ROS quantification

The cytotoxicity of NPs have shown to be associated with the production of ROS; with O_2^- and H_2O_2 being part of the most common ROS produced during normal cellular metabolic processes, and their imbalance under stress yields highly cytotoxic effects (Huang *et al*., 2014). In order to determine the involvement of O_2^- and H_2O_2 upon treatment with MPA-CdTe and carbon QDs, their content in *P. vulgaris* and *G. max* was measured.

4.3.5.1 Superoxide content

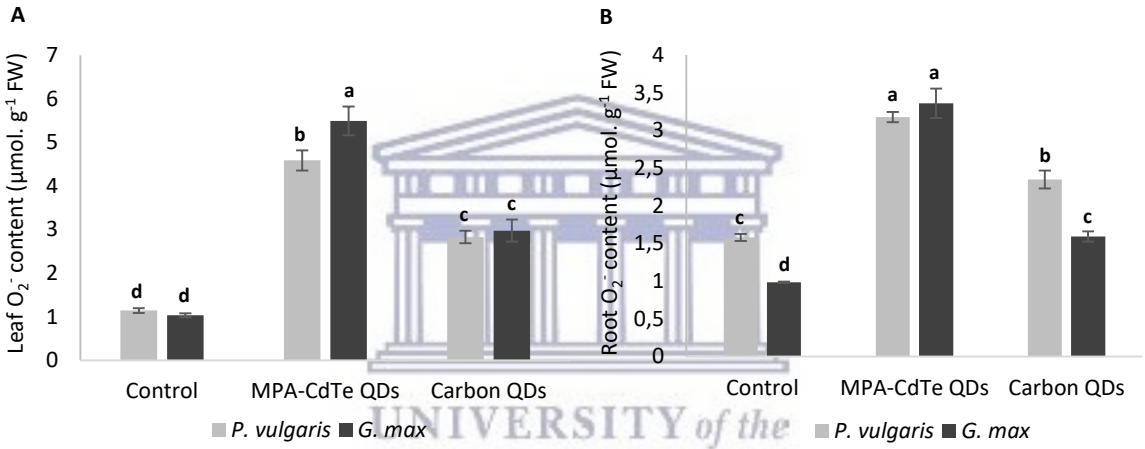

Figure 4: Effect of MPA-CdTe and carbon QDs on O_2^- content in *P. vulgaris* and *G. max*: A) Displays the effect on leaf O_2^- content B) Displays the effect on root O_2^- content. Data represents the mean ±SD (n = 3). Means with the same letter are not significantly different ($p < 0.05$).

In the leaves, upon treatment with MPA-CdTe QDs, the O_2^- content increased by 301.95 % and 430.59 % in *P. vulgaris* and *G. max*, respectively. Likewise, upon treatment with carbon QDs the O_2^- content increased by 147.94 % and 187.33 % in *P. vulgaris* and *G. max* leaves in comparison to respective control plants (Figure 4A). In the roots, a similar trend was observed with a 101.07 % and 240.81 % increase in O_2^- content for *P. vulgaris* and *G. max* upon treatment with MPA-CdTe QDs. For carbon QDs, an increase in 48.72 % and 61.57 % was observed in the roots for *P. vulgaris* and *G. max*, respectively (Figure 4B).

4.3.5.2 Hydrogen peroxide content

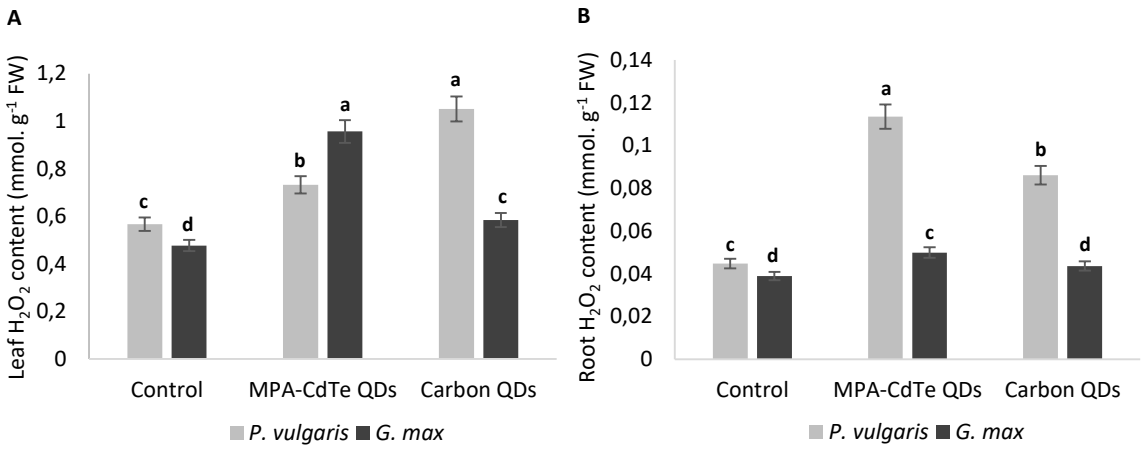

Figure 5: Effect of MPA-CdTe and carbon QDs on H_2O_2 content in *P. vulgaris* and *G. max*: A) Displays the effect on leaf H_2O_2 content B) Displays the effect on root H_2O_2 content. Data represents the mean ±SD (n = 3). Means with the same letter are not significantly different ($p < 0.05$).

A similar trend was observed with regards to H_2O_2 in the leaves and roots of *P. vulgaris* and *G. max* upon treatment with MPA-CdTe and carbon QDs (Figure 5). For *P. vulgaris*, an increase of 29.12 % for MPA-CdTe QDs and 185.36 % in H_2O_2 content was observed for carbon QDs in the leaves. In the roots, H_2O_2 content increased by 156.82 % for MPA-CdTe QDs and 92.82 % for carbon QDs compared to control. Likewise, in *G. max*, an increase of 100.42 % and 22.43 % was exhibited in the leaves for MPA-CdTe and carbon QDs, respectively. In the roots, the H_2O_2 content increased by 28.95 % for MPA-CdTe QDs and 13.16 % for carbon QDs in comparison to the control.

4.3.6 Antioxidant enzyme activity

It is well-known that plants utilize highly complex antioxidant defence systems for protection against oxidative stress, which comprises of antioxidant enzymes such as SOD, CAT and APX. The O_2^- generated from mitochondria, chloroplasts, endoplasmic reticulum, and the cell wall is reduced to H_2O_2 by SOD. The H_2O_2 formed by this reaction is subsequently converted to

H_2O through the activities of CAT and APX (Chen *et al*., 2014). Therefore, the antioxidant enzyme activity in *P. vulgaris* and *G. max* was assessed after treatment with MPA-CdTe and carbon QDs.

4.3.6.1 Superoxide dismutase activity

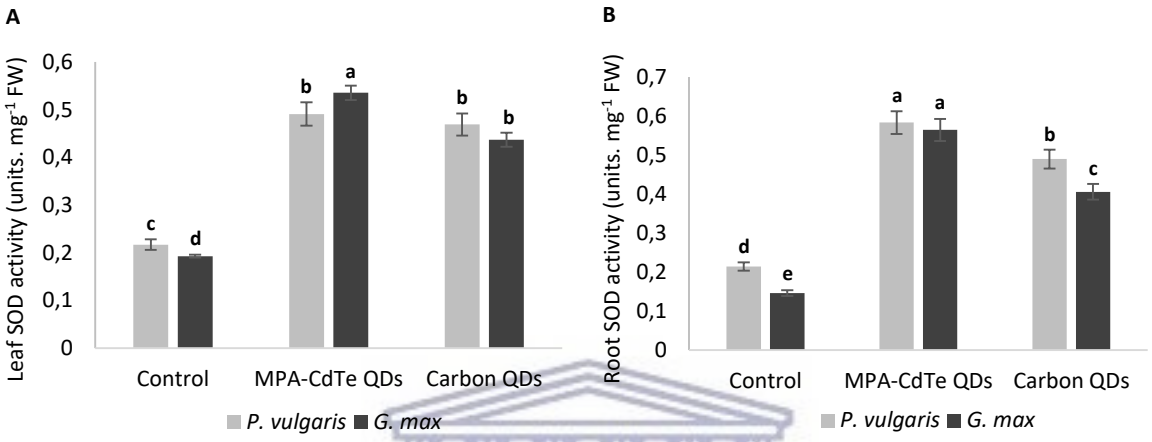

Figure 6: Effect of MPA-CdTe and carbon QDs on SOD activity in *P. vulgaris* and *G. max*: A) Displays the effect on leaf SOD activity B) Displays the effect on root SOD activity. Data represents the mean ±SD (n = 3). Means with the same letter are not significantly different ($p < 0.05$).

In the leaves of *P. vulgaris*, the SOD activity increased by 125.81 % and 115.67 % in comparison to control plants in response to treatment with MPA-CdTe and carbon QDs, respectively. In *G. max*, SOD activity increased by 178.91 % for MPA-CdTe QDs and 127.08 % for carbon QDs (Figure 6A). Similarly, the SOD activity increased in the roots of *P. vulgaris* by 172.43 % and 128.5 % for MPA-CdTe and carbon QDs. In *G. max*, the activity of SOD exhibited an increase of 286.3 % and 177.4 % upon treatment with MPA-CdTe and carbon QDs, respectively (Figure 6B).

4.3.6.2 Catalase activity

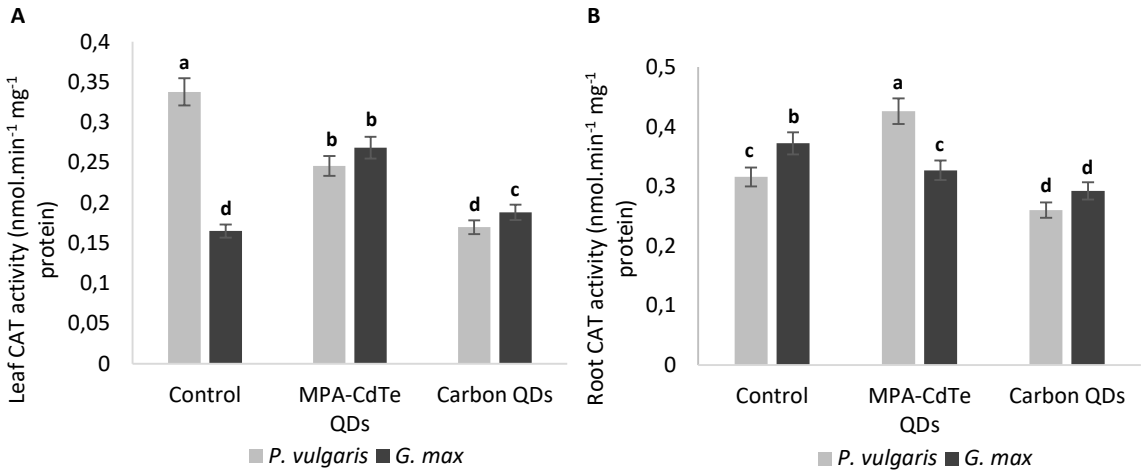

Figure 7: Effect of MPA-CdTe and carbon QDs on CAT activity in *P. vulgaris* and *G. max*: A) Displays the effect on leaf CAT activity B) Displays the effect on root CAT activity. Data represents the mean ± SD (n = 3). Means with the same letter are not significantly different ($p < 0.05$).

Upon treatment with MPA-CdTe and carbon QDs, CAT activity in the leaves of *P. vulgaris* decreased by 27.3 % and 49.85 %, respectively. However, the CAT activity increased by 63.41 % and 14.63 % in the leaves of *G. max* in response to MPA-CdTe and carbon QDs (Figure 7A). In the roots of *G. max*, the CAT activity decreased by 12.3 % for MPA-CdTe QDs and 21.5 % for carbon QDs when compared to the control. Correspondingly, the CAT activity decreased by 17.46 % in the roots for carbon QD treatment in *P. vulgaris*. However, upon treatment with MPA-CdTe QDs the CAT activity increased by 35.24 % in comparison to the control (Figure 7B).

4.3.6.3 Ascorbate peroxidase activity

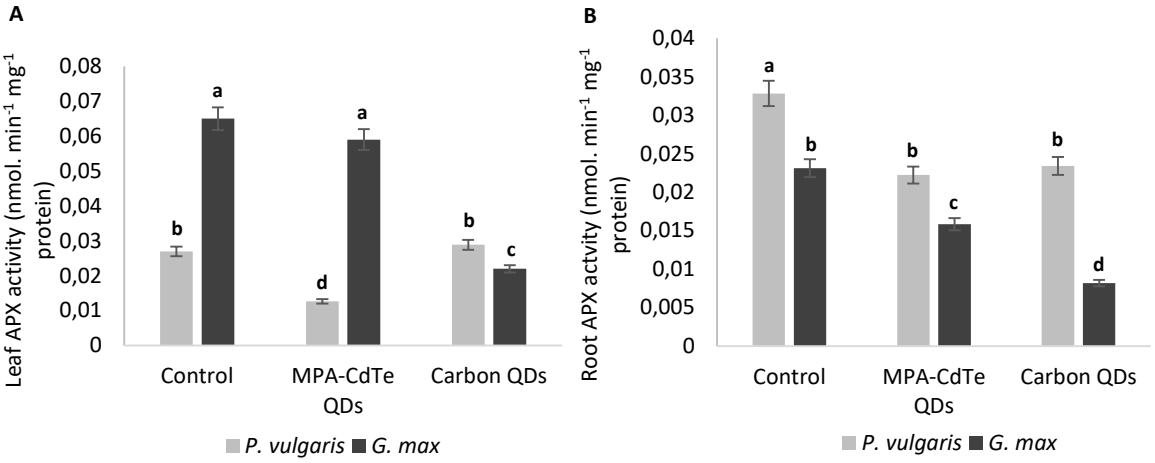

Figure 8: Effect of MPA-CdTe and carbon QDs on APX activity in *P. vulgaris* and *G. max*: A) Displays the effect on leaf APX activity B) Displays the effect on root APX activity. Data represents the mean ± SD (n = 3). Means with the same letter are not significantly different ($p < 0.05$).

In the leaves of *G. max*, a 9.23 % and 67.69 % decrease in APX activity was observed in response to MPA-CdTe and carbon QDs, respectively. Similarly, in *P. vulgaris*, a 53.85 % decrease in response to MPA-CdTe QD treatment, but an increase of 7.69 % was observed with treatment of carbon QDs in comparison to the control (Figure 8A). A similar trend was observed in the roots of both *P. vulgaris*, 31.25 % and 26.88 % decrease, and *G. max*, 34.78 % and 65.22 % decrease, in response to MPA-CdTe and carbon QDs, respectively (Figure 8B).

4.3.7 Macro and micro nutrient assessment by ICP-OES

A balanced content of essential macro and micronutrients plays an important role in the physiological and biochemical functions in plants. Macronutrients are required in large amounts and includes nitrogen (N), phosphorous (P), potassium (K), calcium (Ca) and magnesium (Mg). Micronutrients are required in smaller amounts but are essential for plant growth and includes iron (Fe), zinc (Zn), copper (Cu), manganese (Mn), boron (B), chloride (Cl), molybdenum (Mo) and nickel (Ni) (Panuccio *et al*., 2009).

Table 3: Elemental concentrations (µg. g^{-1}) in the leaves of *P. vulgaris*.

		Control	MPA-CdTe QDs	Carbon QDs
Macronutrients	**K 769.897**	630.55 ^{b}	771.61 ^{a}	655.87 ^{b}
	Ca 396.847	364.41 ^{c}	432.89 ^{b}	508.36 ^{a}
	Mg 280.270	146.20 ^{a}	81.53 ^{c}	119.95 ^{b}
	P 213.618	51.54 ^{a}	48.51 ^{b}	45.07 ^{b}
Micronutrients	**Cu 213.598**	25.48 ^{a}	20.01 ^{b}	14.60 ^{c}
	Zn 213.857	1.76 ^{c}	2.41 ^{a}	1.50 ^{b}
	Mo 202.032	5.76 ^{b}	3.93 ^{c}	6.89 ^{a}
	Mn 257.610	8.93 ^{a}	3.45 ^{c}	7.86 ^{b}
	Fe 238.204	6.67 ^{b}	5.35 ^{c}	7.21 ^{a}

Different letters indicate significant difference between means at $P < 0.05$ (DMRT) per row. Values are means ± SD (n=3). Colour scale from red (decrease) to green (increase).

In the leaves of *P. vulgaris* (Table 3), the concentrations of K and Ca increased by 22.37 % and 18.79 % upon treatment with MPA-CdTe QDs; and 4.01 % and 39.5 % for carbon QDs, respectively. Similarly, the concentrations of Zn increased by 36.93 % with MPA-CdTe QD treatment, and Mo and Fe increased by 19.62 % and 8.1 % respectively with carbon QD treatment. Contrastingly, the concentrations of Mg and P decreased by 44.23 % and 5.88 % with MPA-CdTe QDs, and 17.95 % and 12.55 % with carbon QDs. Likewise, MPA-CdTe QDs resulted in a decrease in Cu by 21.47 %, Mo by 31.77 %, Mn by 61.37 % and Fe by 19.79 %. Upon treatment with carbon QDs the concentrations of Cu, Zn and Mn decreased by 42.7 %, 14.77 % and 11.98 % respectively in comparison to the controls.

Table 4: Elemental concentrations (µg. g^{-1}) in the roots of *P. vulgaris*.

		Control	MPA-CdTe QDs	Carbon QDs
Macronutrients	**K 769.897**	480.35 ^{c}	814.39 ^{a}	672.49 ^{b}
	Ca 396.847	471.80 ^{b}	588.80 ^{a}	388.87 ^{c}
	Mg 280.270	93.33 ^{c}	137.28 ^{a}	120.03 ^{a}
	P 213.618	47.56 ^{b}	57.60 ^{a}	55.63 ^{a}
Micronutrients	**Cu 213.598**	22.60 ^{b}	25.92 ^{a}	28.33 ^{a}
	Zn 213.857	10.35 ^{a}	10.79 ^{a}	12.32 ^{a}
	Mo 202.032	4.68 ^{a}	5.69 ^{a}	6.65 ^{a}
	Mn 257.610	20.69 ^{a}	23.26 ^{a}	25.36 ^{a}
	Fe 238.204	25.11 ^{b}	34.47 ^{a}	27.48 ^{a}

Different letters indicate significant difference between means at P < 0.05 (DMRT) per row. Values are means ± SD (n=3). Colour scale from red (decrease) to green (increase).

In the roots of *P. vulgaris* (Table 4), an increase in macro and micronutrients was observed upon treatment with MPA-CdTe QDs. Concentrations of K, Ca, Mg and P increased by 69.54 %, 24.8 %, 47.1 % and 21.11 %; Cu, Zn, Mo, Mn and Fe increased by 14.69 %, 4.25 %, 21.58 %, 12.42 % and 37.28 %, respectively. In carbon QD-treated plants, the concentrations of K, Mg and P increased by 40 %, 28.61 % and 16.97 %; whereas Ca decreased by 17.58 % in comparison to the control. Similarly, the concentrations of Cu increased by 25.35 %, Zn by 19.03 %, Mo by 42.09 %, Mn by 22.57 % and Fe by 9.44 % with respect to the control *P. vulgaris* plants.

In order to assess the effects of MPA-CdTe and carbon QDs on the translocation of macro and micronutrients between the roots and leaves, the translocation factor for each element was determined (Table 5 & 8). In *P. vulgaris*, a decrease in translocation of K by 27.48 % and 25.19 %, Mg by 62.42 % and 36.94 %, P by 22.22 % and 25 %, Cu by 31.86 % and 53.98 %, Mo by 43.9 % and 15.45 %, and Mn by 65.12 % and 27.91 % in response to treatment with MPA-CdTe and carbon QDs, respectively. Similarly, the movement of Ca decreased by 3.89 % with treatment of MPA-CdTe QDs, but increased by 70.13 % with the treatment of carbon QDs. Whereas, the translocation of Zn increased by 29.41 % with MPA-CdTe QDs and decreased

by 29.41 % with carbon QDs. Furthermore, upon treatment with MPA-CdTe QDs the translocation of Fe decreased by 40.74 %, with no changes observed in the translocation of Fe in *P. vulgaris* upon treatment with carbon QDs (Table 5).

Table 5: Translocation factor of macro and micronutrients in *P. vulgaris*.

		Control	MPA-CdTe QDs	Carbon QDs
Macronutrients	**K 769.897**	1.31 ^{a}	0.95 ^{b}	0.98 ^{b}
	Ca 396.847	0.77 ^{a}	0.74 ^{a}	1.31 ^{a}
	Mg 280.270	1.57 ^{a}	0.59 ^{b}	0.99 ^{b}
	P 213.618	1.08 ^{a}	0.84 ^{b}	0.81 ^{b}
Micronutrients	**Cu 213.598**	1.13 ^{a}	0.77 ^{b}	0.52 ^{b}
	Zn 213.857	0.17 ^{a}	0.22 ^{a}	0.12 ^{a}
	Mo 202.032	1.23 ^{a}	0.69 ^{a}	1.04 ^{b}
	Mn 257.610	0.43 ^{a}	0.15 ^{b}	0.31 ^{a}
	Fe 238.204	0.27 ^{a}	0.16 ^{b}	0.26 ^{a}

Different letters indicate significant difference between means at P < 0.05 (DMRT) per row. Values are means ± SD (n=3).

Table 6: Elemental concentrations (µg. g^{-1}) in the leaves of *G. max*.

		Control	MPA-CdTe QDs	Carbon QDs
Macronutrients	**K 769.897**	767.07 ^{b}	757.72 ^{c}	961.37 ^{a}
	Ca 396.847	245.05 ^{c}	759.95 ^{b}	779.70 ^{a}
	Mg 280.270	115.61 ^{c}	147.76 ^{b}	195.28 ^{a}
	P 213.618	74.68 ^{b}	68.92 ^{c}	94.87 ^{a}
Micronutrients	**Cu 213.598**	38.10 ^{a}	35.68 ^{a}	37.28 ^{b}
	Zn 213.857	3.37 ^{c}	3.96 ^{b}	6.20 ^{a}
	Mo 202.032	0.63 ^{b}	1.53 ^{a}	1.77 ^{a}
	Mn 257.610	6.66 ^{c}	11.42 ^{b}	13.93 ^{a}
	Fe 238.204	10.10 ^{b}	9.74 ^{c}	14.17 ^{a}

Different letters indicate significant difference between means at P < 0.05 (DMRT) per row. Values are means ± SD (n=3). Colour scale from red (decrease) to green (increase).

In the leaves of *G. max* (Table 6), treatment with carbon QDs resulted in an increase in all macronutrients including K, Ca, Mg and P by 25.33 %, 218.18 %, 68.91 % and 27.04 % respectively. Similarly, the concentrations of Zn increased by 83.98 %, Mo by 180.95 %, Mn by 109.16 % and Fe by 40.3 %; whereas Cu decreased by 2.15 %. Upon treatment with MPA-CdTe QDs, K decreased by 1.22 % and P decreased by 7.71 %. Contrastingly, Ca and Mg increased by 210.12 % and 27.81 %. The concentrations of micronutrients including Zn, Mo

and Mn increased by 17.51 %, 142.86 % and 71.47 %, respectively. However, a decrease in the concentrations of Cu by 6.35 % and Fe by 3.56 % was observed in the leaves of *G. max* in response to treatment with MPA-CdTe QDs.

Table 7: Elemental concentrations (µg. g^{-1}) in the roots of *G. max*.

		Control	MPA-CdTe QDs	Carbon QDs
Macronutrients	**K 769.897**	1085.07 ^{b}	1421.60 ^{a}	1375.49 ^{a}
	Ca 396.847	639.61 ^{c}	1252.26 ^{a}	766.87 ^{b}
	Mg 280.270	157.58 ^{b}	230.32 ^{a}	127.26 ^{c}
	P 213.618	113.69 ^{b}	137.09 ^{a}	137.63 ^{a}
Micronutrients	**Cu 213.598**	53.63 ^{b}	62.50 ^{a}	49.90 ^{b}
	Zn 213.857	3.10 ^{b}	4.80 ^{a}	3.52 ^{c}
	Mo 202.032	1.88 ^{c}	2.08 ^{b}	2.48 ^{a}
	Mn 257.610	22.37 ^{b}	33.63 ^{a}	21.76 ^{b}
	Fe 238.204	39.90 ^{c}	66.03 ^{b}	97.90 ^{a}

Different letters indicate significant difference between means at $P < 0.05$ (DMRT) per row. Values are means ± SD (n=3). Colour scale from red (decrease) to green (increase).

In the roots of *G. max* (Table 7), the concentrations of K, Ca and P increased by 31.01 %, 95.78 % and 20.58 % upon treatment with MPA-CdTe QDs; and 26.77 %, 19.9 % and 21.06 % for carbon QDs, respectively. The concentrations of Mg increased by 46.16 % with MPA-CdTe QD treatment and decreased by 19.24 % with carbon QD treatment. Micronutrients including Zn increased by 54.84 % and 13.55 %, Mo by 10.64 % and 21.91 %; and Fe increased by 65.49 % and 145.36 % upon treatment with MPA-CdTe and carbon QDs, respectively. The concentrations of Cu increased by 16.54 % with MPA-CdTe QDs and decreased by 6.96 % with carbon QDs. Similarly, Mn concentrations increased by 50.34 % for MPA-CdTe QD-treatment and decreased by 2.73 % upon treatment with carbon QDs.

In *G. max*, upon treatment with MPA-CdTe QDs, a decrease in translocation was observed for K by 25.35 %, Mg by 12.33 %, P by 24.24 %, Cu by 19.72 %, Zn by 24.77 % and Fe by 40 %. Whereas, the movement of Ca and Mo increased by 60.53 % and 124.24 %, respectively. The translocation of Mn remained unchanged in response to MPA-CdTe QD treatment. In

response to treatment with carbon QDs, an increase in translocation was observed for Ca by 168.42 %, Mg by 109.53 %, P by 4.55 %, Cu by 5.63 %, Zn by 61.47 %, Mo by 118.18 % and Mn by 113.33 %. Contrastingly, Fe decreased by 44 % and K remained unchanged with carbon QD treatment (Table 8).

Table 8: Translocation factor of macro and micronutrients in *G. max*.

		Control	MPA-CdTe QDs	Carbon QDs
Macronutrients	**K 769.897**	0.71 [a]	0.53 [a]	0.7 [a]
	Ca 396.847	0.38 [a]	0.61 [b]	1.02 [a]
	Mg 280.270	0.73 [a]	0.64 [b]	1.53 [a]
	P 213.618	0.66 [a]	0.5 [b]	0.69 [a]
Micronutrients	**Cu 213.598**	0.71 [a]	0.57 [b]	0.75 [a]
	Zn 213.857	1.09 [b]	0.82 [b]	1.76 [a]
	Mo 202.032	0.33 [b]	0.74 [a]	0.72 [a]
	Mn 257.610	0.3 [a]	0.34 [b]	0.64 [a]
	Fe 238.204	0.25 [a]	0.15 [b]	0.14 [b]

Different letters indicate significant difference between means at $P < 0.05$ (DMRT) per row. Values are means ± SD (n=3).

4.4 Discussion

Nanoparticles (NPs) interact with plants producing many morphological and physiological changes which depends on the properties of the NPs; including their chemical composition, size, surface coating, reactivity, and most importantly the concentration at which they are effective. Numerous studies have observed both positive and negative effects on plant growth and development, which have been linked to both the properties of NPs and plant species (Khodakovskaya *et al*., 2012). The role of different NPs on various plants have been studied and most have reported phytotoxic effects. However, most of the reports describe the impact of different NMs at the seedling stage (Priyanka & Venkatachalam, 2016). Therefore, in the present study *P. vulgaris* and *G. max* were grown to a mature growth stage prior to treatment with MPA-CdTe and carbon QDs, and subsequently the physiological and biochemical effects were investigated.

Upon treatment with QDs both *P. vulgaris* and *G. max* displayed a decrease in leaf biomass. However, in *P. vulgaris*, a greater decrease in leaf biomass was observed for carbon QDs of 25.55 %; whereas in *G. max*, MPA-CdTe QDs led to the greatest decrease of 18.51 % in leaf biomass (Figure 1A). Numerous authors have noted a reduction in plant biomass in response to treatment with NPs, Hawthorne et al. (2012) reported that Ag NPs cause biomass reductions up to 49-91 % in *Cucurbita pepo*; De La Torre-Roche et al. (2013) found that the biomass in *G. max* and *Zea mays* was reduced to around 36.5-45 % upon treatment with C_{60} fullerenes; and Asli and Neumann (2009) showed that TiO_2 NPs rapidly inhibited leaf growth in maize.

Contrastingly, in the roots, MPA-CdTe QDs resulted in a decrease in biomass in *G. max* and an increase of 110 % in *P. vulgaris*, and similarly carbon QDs resulted in an increased root biomass in *G. max* but a decreased root biomass in *P. vulgaris* (Figure 1B). Many studies have reported a decrease in root biomass upon treatment with NPs including that reported by Chen et al. (2014), in which the authors observed a reduction in biomass in response to CdTe QDs in wheat seedlings. However, in the present study, a differential response was observed between *P. vulgaris* and *G. max* in response to different types of QDs. Similar findings were reported by Gruyer et al. (2013) as Ag NPs exhibited both positive and negative effects on root elongation depending on the plants species, as they observed that the root length was increased in barley, but inhibited in lettuce. A study by Wang et al. (2014) also showed that rice root growth was markedly increased in comparison to control plants in response to silica-coated QDs. It is proposed that NPs may inhibit plant growth by interrupting stages of cellular metabolism and stages of cell division through the production of excess ROS and peroxidation by-products such MDA (Chichiriccò & Poma, 2015).

Malondialdehyde (MDA) is the decomposition product of polyunsaturated fatty acids of membranes and its increase is the result of greater accumulation under high antioxidant stress. Thus, MDA content serves as an indicator of the extent of lipid peroxidation and an indirect reflection of the extent of cell damage (Wang *et al*., 2011). In the present study, an increase in MDA content was observed in the leaves and roots, but the degree of increase differed between plant species and QD treatment (Figure 2). In *G. max*, the MDA content was the highest in the leaves upon treatment with carbon QDs (52.41 % increase) followed by MPA-CdTe QDs (31.99 % increase). In the roots, MPA-CdTe QDs displayed the largest increase of 45.53 % in MDA in *G. max*. A similar trend was observed in the leaves and roots of *P. vulgaris*, however the level of increase in MDA content was much lower than that experienced in *G. max*. These results are in agreement with those provided by Chen et al. (2014), in which an increase in MDA content was observed with increasing concentrations of CdTe-QDs in wheat. Similarly, upon treatment with CeO_2 NPs, asparagus lettuce roots exhibited a significant increase in MDA content and leakage of electrolytes, which indicated membrane damage in the root cells. It is proposed that NPs cause phytotoxicity through the production of ROS, which subsequently results in oxidative stress, lipid peroxidation, protein and DNA damage and ultimately cell death (Tripathi *et al*., 2017).

Upon treatment with MPA-CdTe and carbon QDs both *P. vulgaris* and *G. max* experienced increased levels of cell death in comparison to their respective controls (Figure 3). However, the extent of cell death in the leaves was greater in *G. max* than *P. vulgaris*, which might explain the increased MDA content observed in the leaves of *G. max* (Figure 2A). Similarly, the large increase in cell death of 528.75 % experienced by *G. max* in response to MPA-CdTe QDs correlates to the increase in MDA content in the roots (Figure 2B & 3B). It is also important to note that the degree of cell death experienced in the roots was far greater than

that experienced in leaves of *P. vulgaris* and *G. max*. Similar findings were observed in the roots of eggplant in which cobalt oxide NPs (CoO NPs) induced cell death via mitochondrial membrane damage and subsequent swelling (Faisal *et al*., 2016). Faisal et al. (2013) reported an increase in apoptotic and necrotic cells in the roots of tomato in response to nickel oxide NPs (NiO NPs). Lin, S et al. (2009) also reported the phytotoxic effect of multi-walled carbon nanotubes in *Oryza sativa* and Lin, C et al. (2009) in *A. thaliana*. Moreover, NPs such as CeO_2 and TiO_2 NPs have been linked to disorganized DNA and damage to DNA structure in *G. max* and *Zea mays* (Lopez-Moreno *et al*., 2010; Castiglione *et al*., 2011). It is proposed that after the accumulation of NPs in plants, it results in the enhancement of chromatin condensation, increased DNA damage, reduction in the rate of transpiration, increased lipid peroxidation, up and down regulation of various stress related genes and lastly apoptosis (Tripathi *et al*., 2017).

A study conducted by Chen et al. (2014) observed that treatment of wheat seedlings with CdTe QDs resulted in a decrease in chlorophyll *a*, *b* and total chlorophyll concentrations. Those findings are in agreement with the results obtained in this study as MPA-CdTe QDs caused a reduction in chlorophyll *a*, *b* and total chlorophyll content in both *P. vulgaris* and *G. max* (Table 1 & 2). It is suggested that the decrease in chlorophyll content in plants could be as a result of the temporary inhibition of photosynthesis, increased respiration and reduced transpiration, and a considerable loss of intracellular potassium (Fatoba & Emem, 2008; Tripathi *et al*., 2017). Contrastingly, an increase in chlorophyll *a* and *b* was observed in *P. vulgaris* and *G. max* in response to treatment with carbon QDs. Priyanka and Venkatachalam (2016) reported increased levels of photosynthetic pigment contents, including chlorophyll *a*, *b* and carotenoids in the leaves of the cotton plants after treatment with ZnO NPs; and the increase correlated to an increasing NP concentration. Similarly, Gopinath et al. (2014)

reported that Au NPs improved the number of leaves, leaf area and chlorophyll content in *Gloriosa superba*.

It has become widely accepted that NPs are either directly or indirectly involved in the overproduction of ROS, which triggers the activation of ROS scavenging mechanisms (Tripathi *et al*., 2017). If ROS are not effectively scavenged it will result in oxidative stress, lipid peroxidation, protein oxidation, chlorosis, and damage to DNA, ultimately leading to cell death (Arruda *et al*., 2015). One of the first ROS molecules generated under stress is O_2^- (Gill & Tuteja, 2010). Upon quantification of O_2^- in the leaves and roots of *P. vulgaris* and *G. max*; an increase in O_2^- was observed in response to both MPA-CdTe and carbon QD treatment (Figure 4). Chen et al. (2014) reported similar findings in which CdTe QDs resulted in a marked increase in the concentrations of O_2^- in the roots and shoots of *Triticum aestivum* L. In the present study, MPA-CdTe QDs caused a higher increase in both plants species in comparison to carbon QDs. Furthermore, *G. max* experienced a larger increase in O_2^- content in the leaves and roots in comparison to *P. vulgaris*.

Within plant cells, SOD constitutes the first line of defence against ROS by catalysing the dismutation of O_2^- (Santos *et al*., 2013). Upon treatment with MPA-CdTe and carbon QDs, *P. vulgaris* and *G. max* experienced an increase in SOD activity in the leaves and roots (Figure 6). These findings are in accordance to those reported by Raskar & Laware (2014) in which onion seedlings clearly exhibited an increase in activity of SOD with increasing TiO_2 NP concentrations. Similarly, Santos et al. (2013) observed a 12 %, 27 % and 88 % increase in SOD activity when *M. sativa* cells were exposed to 10, 50 and 100 nM of MPA-CdSe/ZnS QDs, respectively. It is important to note, that MPA-CdTe QDs resulted in the highest increase in O_2^- content (Figure 4), which may be responsible for the large increase in SOD activity

experienced in the leaves and roots of *P. vulgaris* and *G. max* in response to MPA-CdTe QD treatment (Figure 6A & 6B).

As mentioned previously, SOD is the first enzymatic defence that acts against ROS to convert O_2^- to less toxic H_2O_2 and O_2 (Priyanka & Venkatachalam, 2016). Thus, another important ROS molecule is H_2O_2; at low concentrations, it acts as a signalling molecule that aids in tolerance to various stresses, and at higher concentrations, it contributes to cell death (Quan *et al*., 2008). Similar to that observed by Chen et al. (2014), an increase in leaf and root H_2O_2 was observed in *P. vulgaris* and *G. max* in response to treatment with MPA-CdTe and carbon QDs (Figure 5). Interestingly, MPA-CdTe QDs resulted in the highest level of H_2O_2 in the leaves of *G. max*, whereas *P. vulgaris* experienced the highest increase of 185.36 % in H_2O_2 upon treatment with carbon QDs. Furthermore, in the roots, *P. vulgaris* displayed the highest increase in H_2O_2 content upon treatment with MPA-CdTe and carbon QDs when compared to *G. max*. This may be as a result of the higher activity of SOD and subsequent generation of more H_2O_2 molecules in the roots (Figure 6).

It has been recognised that an excess production of H_2O_2 in plant cells leads to oxidative stress (Gill & Tuteja, 2010). CAT and APX are notable antioxidant defence enzymes involved in the detoxification of H_2O_2 by converting free radicals to H_2O and O_2 (Bowler *et al*., 1992). In the leaves of *G. max*, treatment with MPA-CdTe and carbon QDs resulted in an increase in CAT activity and decrease in APX activity (Figure 7A & 8A). Santos et al. (2013) observed an increased CAT activity in *M. sativa* cells in response to treatment with MPA-CdSe/ZnS QDs. Moreover, the low activity of APX may be attributed to the remarkable activity of CAT as a key enzyme in the elimination of H_2O_2 (Ghanati *et al*., 2005). In the roots of *G. max*, a decrease in CAT and APX activity was observed (Figure 7B & 8B). These findings are similar to

those reported by Chen et al. (2014), in which the toxicity in the roots was manifested as a result of decreased antioxidant enzyme activities including CAT and APX upon treatment with CdTe QDs in wheat seedlings. Similarly, Kim et al. (2012) reported decreased CAT activity in ZnO NP treated *Cucumis sativus* plants. A decrease in CAT and APX activity may have contributed to toxicity in *G. max* and may have attributed to the increase in cell death observed in the roots (Figure 3). In *P. vulgaris*, treatment with carbon QDs resulted in a decrease in CAT activity and an increase in APX activity in the leaves. Whereas, treatment with MPA-CdTe QDs resulted in a decrease in activities of both CAT and APX, possibly contributing to the lower chlorophyll concentrations and, increased lipid peroxidation and cell death. In the roots of *P. vulgaris*, an increase in CAT activity and a decrease in APX activity was observed in response to treatment with MPA-CdTe QDs; and decrease in APX and CAT activities in response to treatment with carbon QDs which may have contributed to the high level of cell death and decrease in root biomass (Figure 1B & 3B).

A number of reports have demonstrated that due to their small size, NMs pass biological barriers and may induce physiological, biochemical and genetic modifications in plants (Gardea-Torresdey *et al*., 2014). Therefore, the investigation of further potential negative effects concerning the modifications on crop nutritional content is imperative, as it is strongly related to food nutritional value and human health (Mattiello *et al*., 2016). For this reason, the macro and micronutrient accumulation in the leaves and roots of *P. vulgaris* (Table 3 & 4) and *G. max* (Table 6 & 7) was assessed after exposure to MPA-CdTe and carbon QDs using ICP-OES.

In the leaves and roots of *P. vulgaris*, K concentration increased with treatment of MPA-CdTe and carbon QDs. In *G. max*, treatment with carbon QDs resulted in increased K concentration

in the leaves and roots, whereas treatment with MPA-CdTe QDs resulted in an increase in the roots but a decrease in the leaves. Furthermore, even though the concentration of K increased within the roots of *P. vulgaris* and *G. max*, the translocation of K from the roots to leaves decreased (Table 5 & 8). In plant cell metabolism, K is involved in protein synthesis, in maintaining the osmotic potential, and controlling the pH equilibrium (Mattiello *et al*., 2016), a reduction of K concentration in plants might have a negative impact on enzyme activities and, therefore, on nutritional quality.

In the leaves of *P. vulgaris*, Ca concentration increased upon treatment with MPA-CdTe and carbon QDs, whereas Mg concentration decreased upon treatment. In the roots of *P. vulgaris*, the Mg concentration decreased with both QD treatments; whereas the concentration of Ca increased upon treatment with MPA-CdTe QDs and decreased with carbon QDs (Table 4). Furthermore, in *G. max*, the concentrations of Ca and Mg increased in the leaves in response to treatment with MPA-CdTe and carbon QDs. A study by Rico et al. (2013), showed CeO_2 NPs caused an increase in Ca concentration by 25.5 % in comparison to untreated *Oryza sativa* L. (rice) plants. In the roots of *G. max*, Ca concentration increased with MPA-CdTe and carbon QD treatment, and Mg concentration decreased with MPA-CdTe QD treatment but increased with carbon QD treatment (Table 7).

Moreover, the translocation of Ca increased in *G. max* in response to treatment with MPA-CdTe and carbon QDs; but only increased for carbon QD treatment and decreased in response to MPA-CdTe QDs in *P. vulgaris*. Similarly, Mg translocation decreased in response to treatment with MPA-CdTe QDs and decreased with carbon QDs in *G. max*. Whereas, in *P. vulgaris* the translocation of Mg between the roots and leaves decreased upon treatment with MPA-CdTe and carbon QDs (Table 5). Similar findings were reported by Zuverza-Mena

et al. (2016), in which Ag NPs reduced the uptake of macro-elements including Ca and Mg in radish, and proposed that NPs may decrease the expression of the Ca channel protein, reducing Ca uptake; and it is very likely that at high concentrations, NPs may also aggregate and physically block the channels, thereby reducing the absorption of Mg. A reduction in Mg translocation may pose a serious problem, as Mg is particularly important in plants; with approximately 75 % of leaf Mg involved in protein synthesis and about 15-20 % of total Mg associated with chlorophyll pigments, where it acts mainly as a cofactor for a series of enzymes involved in photosynthetic carbon fixation and metabolism (Guo *et al*., 2016).

Phosphorus (P) is one of the essential macro-elements required for plant growth and development (Vance *et al*., 2003), and plays a pivotal role in many crucial processes including energy metabolism and phosphorylation-based signalling mechanisms (Nussaume *et al*., 2011). In the present study, P concentrations increased in the roots of both *P. vulgaris* and *G. max* in response to treatment with MPA-CdTe and carbon QDs (Table 4 & 7). These findings are in agreement with those reported by Rico et al. (2014), in which CeO_2 NPs resulted in an increased concentration of P in the roots of wheat plants. However, despite the increase in P concentrations in the roots observed in *P. vulgaris* and *G. max*, the translocation of P decreased with respect to the control plants. This decrease in P translocation in plants, between organs and subcellular compartments, may be as a result of the interference of NPs with the binding of inorganic phosphate to phosphate transporters or the co-ordination of a set of proteins involved in P transport activities (Gu *et al*., 2016).

Micronutrients play a significant role in plant growth and metabolic processes associated with photosynthesis, chlorophyll formation, cell wall development and respiration, water absorption, xylem permeability, resistance to plant diseases, enzyme activities, and nitrogen

fixation and reduction (Adhikary *et al*., 2010). In plants, Fe acts as a catalyst for chlorophyll biosynthesis, as an oxygen carrier and aids in respiratory enzyme systems (Monreal *et al*., 2015). In the present study, treatment with MPA-CdTe and carbon QDs caused an increase in Fe concentrations in the roots of both *P. vulgaris* and *G. max*, and an increase in the leaves of *P. vulgaris* and *G. max* upon treatment with carbon QDs. However, a decrease in Fe concentrations was observed in the leaves of *P. vulgaris* and *G. max* in response to treatment with MPA-CdTe QDs. This coupled with the decrease in translocation of Fe observed between the roots and the leaves of *P. vulgaris* (Table 5) and *G. max* (Table 8), may be responsible for the decrease in chlorophyll *a* and *b* concentrations experienced in both plants upon treatment with MPA-CdTe QDs (Table 1 & 2). It has been reported that Fe-deficiency leads to a decrease in the chlorophyll concentration, which affects the photosynthetic metabolism and the development of plants as photosynthetic efficiency; and the structure and function of the photosynthetic apparatus is highly Fe-dependent (Pariona et *al*., 2016).

Cu is involved in several enzyme systems, cell wall formation, electron transport and oxidation reactions (Monreal *et al*., 2015). In *P. vulgaris*, Cu concentrations increased in the roots but decreased in the leaves; which may be a direct result of the decrease in Cu translocation between the roots and leaves in response to treatment with MPA-CdTe and carbon QDs (Table 5). Similarly, in *G. max*, treatment with MPA-CdTe QDs resulted in increased Cu concentrations in the roots but decreased Cu concentrations in the leaves.

Similar to most metals required for plant growth, Mo has been utilized by specific plant enzymes to participate in reduction and oxidation reactions (Kaiser *et al*., 2005). This element is crucial for the functions of nitrogenase and nitrate reductase, two enzymes important for nitrogen fixing and nitrogen reduction. In addition, Mo is especially important in legumes as

they rely heavily upon a symbiotic bacterium to fix nitrogen (Purvis, 1955). In the roots of *P. vulgaris* and *G. max*, the concentration of Mo increased with the treatment of MPA-CdTe and carbon QDs. Similarly, an increase in concentration of Mo was observed in the leaves of *G. max* with QD-treatment (Table 6). Whereas, upon treatment with carbon QDs, Mo concentrations increased but decreased with MPA-CdTe QD- treatment in *P. vulgaris* (Table 3). Zhang et al. (2014), also reported a decrease in Mo concentrations in cucumber plants after exposure to CeO_2 NPs and ZnO NPs.

As a co-factor, Zn is involved in a number of enzyme systems, metabolic reactions and is necessary for the production of chlorophyll and carbohydrates (Monreal *et al*., 2015). In the present study, treatment with MPA-CdTe and carbon QDs led to an increase in Zn concentrations in the roots of *P. vulgaris* and *G. max*; and the leaves of *G. max* in response to QD-treatment. In the leaves of *P. vulgaris*, Zn concentrations increased by 36.93 % upon treatment with MPA-CdTe QDs but decreased by 14.77 % with carbon QD treatment. Zn deficiency results in multiple symptoms including leaves developing brown blotches and streaks that may fuse to cover older leaves entirely, plants remain stunted, bud development becomes poor resulting in reduced flowering and branching, and in severe cases plants may die (Wissuwa *et al*., 2006).

Mn activates several important metabolic reactions, aids in chlorophyll synthesis, and photosynthesis (Monreal *et al*., 2015). In the present study, Mn concentrations decreased in response to MPA-CdTe and carbon QD treatment (Table 3). Moreover, Mn concentrations increased in the leaves of *G. max* and in the roots of *P. vulgaris* with MPA-CdTe and carbon QD treatments. Trujillo-Reyes et al. (2014) reported changes in the accumulation of Mn and Zn in lettuce leaves exposed to core-shell Fe/Fe_3O_4 and Cu/CuO NPs. In the roots of *G. max*,

MPA-CdTe QD treatment caused an increase in Mn and carbon QD treatment caused a decrease in Mn concentration in comparison to the control (Table 7). In *P. vulgaris*, Zn translocation increased with MPA-CdTe QDs and decreased with carbon QD treatment. Similarly, the movement of Mn decreased in response to treatment with MPA-CdTe and carbon QDs (Table 5). In *G. max*, treatment with carbon QDs increased the translocation of Zn and Mn between the roots and leaves (Table 8). However, in response to treatment with MPA-CdTe QDs the translocation of Zn decreased and Mn remained unchanged. The uptake of Zn and Mn by roots is mediated by zinc-regulated transporter/iron-regulated transporter (*ZRT/IRT1*)-related protein (*ZIP*) transporters and natural resistance-associated macrophage protein (*Nramp*) transporters (Mukherjee *et al*., 2016). At this point, the current information is not sufficient to develop a clear idea of how NPs could affect the uptake of macro and microelements in terms of their interaction with specific metal transporters or the genes encoding for metal transporters. As explained above, it is also possible that NPs may physically block the diffusion pathway or the channels responsible for active absorption (Zuverza-Mena *et al*., 2016).

Conclusion and Future Work

The results of this study indicates that intact MPA-CdTe and carbon QDs were taken up from the soil by the roots of *P. vulgaris* and *G. max* and translocated to the leaves and in addition to the bean pods of *P. vulgaris*. Thus, providing evidence of a potential route for QDs to enter the food web. It is important to note that the extent of translocation and degree of accumulation in plant structures differed between plants and QD-type. How NPs enter plant cells and are distributed to different plant structures, how they affect growth or yield, and the associated modes of action are yet to be understood. Many studies have suggested that NPs can translocate via xylem in an upward movement and phloem in a downward movement, but how NPs cross plant cell membranes; whether they use some transporters/channels; whether they move using symplastic or apoplastic pathways, are questions that are yet to be answered and that may differ between NP type and plant genotype.

A large number of studies have reported that NPs cause phytotoxic effects in plants. The present study shows similar findings as MPA-CdTe and carbon QDs initiated oxidative stress in *P. vulgaris* and *G. max*; as many physiological changes including increased lipid peroxidation and cell death; altered chlorophyll *a* and *b* concentrations and plant biomass was observed. Biochemical changes included increased levels of ROS including H_2O_2 and O_2^- and the activation of multiple antioxidant enzymes such as SOD, CAT and APX, which are known to alleviate NP toxicity in plants. Despite the lower toxicity and increased biocompatibility of carbon QDs in comparison to MPA-CdTe QDs; they still possessed the ability to induce oxidative stress in *P. vulgaris* and *G. max*. Furthermore, the extent of damage was greater in *G. max* than in *P. vulgaris*, suggesting that *P. vulgaris* may be more tolerant or

may possess mechanisms to better cope under stress than *G. max*. It is evident from the compiled information that the manner in which NPs interact with cellular moieties to induce excess ROS generation and the subsequent antioxidative mechanisms is a matter of conjecture. However, it is clear that the effects of NPs varies from plant to plant and depends on the NP size and type.

In terms of cellular uptake and transport, there are a number of different transporter genes and pathways present, which regulates the mobility of different elements across the plasma membrane. It is clear from this study that even though a number of macro and microelement concentrations in the roots of *P. vulgaris* and *G. max* increased, yet the overall translocation between roots, shoots and leaves decreased. A decrease in translocation and accumulation of important elements that are required for plant growth and development, may have detrimental impact crop productivity and yield as well as negative implications on overall food quality.

In order to further validate and justify the findings of this study, a more comprehensive analysis should be performed. This will be achieved by assessing damage to DNA using Comet's assay and DNA laddering/fragmentation, which is a feature of apoptosis in order to investigate programmed cell death. In addition, antioxidant enzyme activity will be further validated using native-PAGE analysis in order to identify the APX and SOD isoforms that are up or down-regulated in response to QD stress. The content and activity of plant hormones including indole-3-acetic acid (IAA), abscisic acid (ABA) and gibberellic acid (GA) will be assessed as they are considered an important index of toxicity in plants. Confocal and HR-TEM microscopy can be used to visualise the pattern of distribution and accumulation of QDs at a cellular level as well as track the movement and pathway that QDs utilize within each

cell and between cells. Furthermore, confocal imaging can be used to assess plant cell morphology in order to detect features of programmed cell death. Fourier transform infrared (FT-IR) spectroscopy has been used to identify conformational changes in the macromolecules of plants exposed to contaminants, including NPs and will be used to investigate the amino acid content, lipid and carbohydrate profiles in the beans of *P. vulgaris* and *G. max* after exposure to QDs; as NPs can have significant and contrasting impacts on the composition and nutritional value of crop plants.

The above mentioned work may provide a more clear view of the impact and toxicity of QDs in plants. However, it is clear that the interaction between plants and NPs is highly complex and depends on factors including NP shape, size, surface features, crystal chemistry, dose, etc. as well as: plant genotype and age, soil or growth supporting medium, and the route of exposure. Thus, the obtained scientific knowledge still needs further inspection and more studies should focus on nanotoxicity, especially in a variety of plant systems, in order to fully understand the benefits and risks surrounding NPs; and to build suitable databases with regards to its safety and toxicity. In addition, a series of safety evaluation and toxicological risk assessment standards should be formulated, in order to provide a scientific basis for the application of NPs before it can be applied in industry. As the uncontrolled release and accumulation of NPs into the environment and subsequently in plants will result in its movement through different trophic levels in an ecosystem and may negatively impact environmental and human health.

References

Adhikary, B. H., Shrestha, J., & Baral, B. R. (2010). Effects of micronutrients on growth and productivity of maize in acidic soil. *International Research Journal of Applied and Basic Sciences*, 1, 8-15.

Arora, S., Sharma, P., Kumar, S., Nayan, R., Khanna, P. K., & Zaidi, M. G. (2012). Gold-nanoparticle induced enhancement in growth and seed yield of *Brassica juncea*. *Plant Growth Regulation*, 66, 303-310.

Arruda, S. C., Silva, A. L., Galazzi, R. M., Azevedo, R. A., & Arruda, M. A. (2015). Nanoparticles applied to plant science: a review. *Talanta*, 131, 693-705.

Asli, S., & Neumann, P. M. (2009). Colloidal suspensions of clay or titanium dioxide nanoparticles can inhibit leaf growth and transpiration via physical effects on root water transport. *Plant, Cell & Environment*, 32(5), 577-584.

Atha, D. H., Wang, H., Petersen, E. J., Cleveland, D., Holbrook, R. D., Jaruga, P., Nelson, B. C. (2012). Copper oxide nanoparticle mediated DNA damage in terrestrial plant models. *Environmental Science & Technology*, 46(3), 1819-1827.

Banerjee, A., Pons, T., Lequeux, N., & Dubertet, B. (2016). Quantum dots-DNA bioconjugates: synthesis to applications. *Interface Focus*, 6, 1-17.

Bao-shan, L., Shao-qi, D., Chun-hui, L., Li-jun, F., Shu-chun, Q., & Min, Y. (2004). Effect of TMS (nanostructured silicon dioxide) on growth of *Changbai larch* seedlings. *Journal of Forestry Research*, 15, 138-140.

Barka, E. A. (2001). Protective enzymes against reactive oxygen species during ripening of tomato (*Lycopersicon esculentum*) fruits in response to low amounts of UV-C. *Australian Journal of Plant Physiology*, 28, 785–791.

Batley, G. E., Kirby, J. K., & McLaughlin, M. J. (2013). Fate and risks of nanomaterials in aquatic and terrestrial environments. *Accounts of Chemical Research*, 46, 854-862.

Beattie, I. R., & Haverkamp, R. G. (2011). Silver and gold nanoparticles in plants: Sites for the reduction to metal. *Metallomics*, 3(6), 628-632.

Bowler, C., Van Montague, M., & Inze, D. (1992). Superoxide dismutase and stress tolerance. *Annual Review of Plant Molecular Biology*, 43, 83-116.

Cabiscol, E., Tamarit, J., & Ros, J. (2010). Oxidative stress in bacteria and protein damage by reactive oxygen species. *International Microbiology*, 3(1), 3-8.

Castiglione, M. R., Giorgetti, L., Geri, C., & Cremonini, R. (2011). The effects of nano-TiO2 on seed germination, development and mitosis of root tip cells of *Vicianar bonensis* L. and *Zea mays* L. *Journal of Nanoparticle Research*, 13(6), 2443-2449.

Chakravarty, D., Erande, M. B., & Late, D. J. (2015). Graphene quantum dots as enhanced plant growth regulators: effects on coriander and garlic plants. *Journal of the Science of Food and Agriculture*, 95(3), 2772-2778.

Chen, H., Gong, Y., & Han, R. (2014). Cadmium Telluride Quantum Dots (CdTe-QDs) and Enhanced Ultraviolet-B (UV-B) Radiation Trigger Antioxidant Enzyme Metabolism and Programmed Cell Death in Wheat Seedlings. *PLOS ONE*, 9(10), 1-13.

Chen, N., He, Y., Li, X., Huang, Q., Wang, H., Zhang, X., & Fan, C. (2012). The cytotoxicity of cadmium-based quantum dots. *Biomaterials*, 33(5), 1238-1244.

Chichiriccò, G., & Poma, A. (2015). Penetration and Toxicity of Nanomaterials in Higher Plants. *Nanomaterials*, 5, 851-873.

Cho, S. J., Maysinger, D., Jain, M., Roder, B., Hackbarth, S., & Winnik, F. M. (2007). Long-term exposure to CdTe quantum dots causes functional impairments in live cells. *Langmuir*, 23(4), 1974-1980.

Chomoucka, J., Drbohlavova, J., Vaculovicova, M., Businova, P., Prasek, J., Pekarek, J., & Hubalek, J. (2013). Study of Protein Conjugation with Different Types of CdTe Quantum Dots. ISBN: 978-1-61208-303-2.

Cifuentes, Z., Custardoy, L., de la Fuente, J. M., Marquina, C., Ibarra, M. R., Rubiales, D., & Alejandro Pérez-de-Luque, A. (2010). Absorption and translocation to the aerial part of magnetic carbon-coated nanoparticles through the root of different crop plants. *Journal of Nanobiotechnology*, 8.

Cornelis, G., Hund-Rinke, K., Kuhlbusch, T., Van den Brink, N., & Nickel, C. (2014). Fate and bioavailability of engineered nanoparticles in soils: a review. *Critical Reviews in Environmental Science and Technology*, 44, 2720-2764.

Cui, D., Zhang, P., Ma, Y., He, X., Li, Y., Zhang, J., & Zhang, Z. (2014). Effect of cerium oxide nanoparticles on asparagus. *Environmental Science Nano*, 1, 459-465.

de la Rosa, G., Lopez-Moreno, M. L., de Haro, D., Botez, C. E., Peralta-Videa, J. R., & Gardea-Torresdey, J. L. (2013). Effects of ZnO nanoparticles in alfalfa, tomato, and cucumber at the germination stage: root development and X-ray absorption spectroscopy studies. *Pure and Applied Chemistry*, 85(12), 2161-2174.

De La Torre-Roche, R., Hawthorne, J., Deng, Y., Xing, B., Cai, W., Newman, L. A., & White, J. C. (2013). Multiwalled carbon nanotubes and C60 fullerenes differentially impact the accumulation of weathered pesticides in four agricultural plants. *Environmental Science & Technology*, 47(21), 12539-12547.

dos Santos Soares, A. M., de Souza, T. F., Jacinto, T., & Tavares Machado, O. L. (2010). Effect of Methyl Jasmonate on antioxidative enzyme activities and on the contents of ROS and H_2O_2 in *Ricinus communis* leaves. *Brazilian Society of Plant Physiology*, 22(3), 151-158.

Duan, J., Song, L., & Zhan, J. (2009). One-Pot Synthesis of Highly Luminescent CdTe Quantum Dots by Microwave Irradiation Reduction and Their Hg^{2+} Sensitive Properties. *Nano Research*, 2, 61-68.

Faisal, M., Saquib, Q., Alatar, A. A., Al-Khedhairy, A. A., Ansari, S. M., Alwathnani, H. A., & Praveen, S. (2016). Cobalt oxide nanoparticles aggravate DNA damage and cell death in eggplant via mitochondrial swelling and NO signalling pathway. *Biological Research*, 49(20), 1-13.

Faisal, M., Saquib, Q., Alatar, A. A., Al-Khedhairy, A. A., Hegazy, A. K., & Musarrat, J. (2013). Phytotoxic hazards of NiO-nanoparticles in tomato: A study on mechanism of cell death. *Journal of Hazardous Materials*, 250, 318-332.

Fatoba, P. O., & Emem, U. G. (2008). Effects of Some Heavy Metals on Chlorophyll Accumulation in *Barbula lambarenensis*. *Ethnobotanical Leaflets*, 12, 776-783.

Frasco, M. F., & Chaniotakis, N. (2009). Semiconductor Quantum Dots in Chemical Sensors and Biosensors. *Sensors*, 9, 7266-7286.

Garcia-Limones, C., Hervas, A., Nava-Cortes, J. A., Jimenez-Diaz, R. M., & Tena, M. (2002). Induction of an antioxidant enzyme system and oxidative stress markers associated with compatible and incompatible interactions between chickpea (*Cicer arietinum* L.) and *Fusarium oxysporum* f. sp. *ciceris*. *Physiological and Molecular Plant Pathology*, 61, 325-337.

Gardea-Torresdey, J. L., Gomez, E., Peralta-Videa, J. R., Parsons, J. G., Troiani, H., & Jose-Yacaman, M. (2003). Alfalfa sprouts: A natural source for the synthesis of silver nanoparticles. *Langmuir*, 19(4), 1357-1361.

Gardea-Torresdey, J. L., Rico, C. M., & White, J. C. (2014). Trophic transfer, transformation and impact of engineered nanomaterials in terrestrial environments. *Environmental Science & Technology*, 48, 2526-2540.

Ghanati, F., Morita, A., & Yokota, H. (2005). Effects of aluminum on the growth of tea plant and activation of antioxidant systems. *Plant and Soil*, 276, 133-141.

Ghosh, M., Bandyopadhyay, M., & Mukherjee, A. (2010). Genotoxicity of titanium dioxide (TiO_2) nanoparticles at two trophic levels: plant and human lymphocytes. *Chemosphere*, 81, 1253-1262.

Gill, S. S., & Tuteja, N. (2010). Reactive oxygen species and antioxidant machinery in abiotic stress. *Plant Physiology and Biochemistry*, 1-22.

Gopalakrishnan Nair, P. M., & Chung, I. M. (2014). Assessment of silver nanoparticle-induced physiological and molecular changes in *Arabidopsis thaliana*. *Environmental Science and Pollution Research*, 21(14), 8858-8869.

Gopinath, K., Gowri, S., Karthika, V., & Arumugam, A. (2014). Green synthesis of gold nanoparticles from fruit extract of *Terminalia arjuna*, for the enhanced seed germination activity of *Gloriosa superba*. *Journal of Nanostructure in Chemistry*, 4, 1-11.

Gottschalk, F., Sonderer, T., Scholz, R. W., & Nowack, B. (2009). Modelled environmental concentrations of engineered nanomaterials (TiO_2, ZnO, Ag, CNT, fullerenes) for different regions. *Environmental Science & Technology*, 43, 9216-9222.

Gruyer, N., Dorais, M., Bastien, C., Dassylva, N., & Triffault-Bouchet, G. (2013). Interaction between silver nanoparticles and plant growth. In International symposium on new technologies for environment control, energy-saving and crop production in greenhouse and plant factory - greensys (pp. 6-11). Jeju, Korea.

Gu, M., Chen, A., Sun, S., & Xu, G. (2016). Complex Regulation of Plant Phosphate Transporters and the Gap between Molecular Mechanisms and Practical Application: What Is Missing?, *Molecular Plant*, 9, 396-416.

Guo, W., Hussain, N., Liang, Z., & Yang, D. (2016). Magnesium deficiency in plants: An urgent problem, *The Crop Journal*, 4(2), 83-91.

Havlin, J. L., & Soltanpour, P. N. (2006). A nitric acid plant tissue digest method for use with inductively coupled plasma spectrometry. *Communications in Soil Science and Plant Analysis*, 11(10), 969-980.

Hawthorne, J., Musante, C., Sinha, S. K., & White, J. C. (2012). Accumulation and phytotoxicity of engineered nanoparticles to *Cucurbita pepo*. *International Journal of Phytoremediation*, 14(4), 429-442.

Hong, F., Zhou, J., Liu, C., Yang, F., Wu, C., Zheng, L., & Yang, P. (2005). Effect of nano-TiO_2 on photochemical reaction of chloroplasts of spinach. *Biological Trace Element Research*, 105(1-3), 269-279.

Hoshino, A., Fujioka, K., Oku, T., Suga, M., Sasaki, Y. F., Ohta, T., & Yamamoto, K. (2004). Physicochemical Properties and Cellular Toxicity of Nanocrystal Quantum Dots Depend on Their Surface Modification. *Nano Letters*, 4(11), 2163-2169.

Huang, W., Yang, X., Yao, S., LwinOo, T., & He, H. (2014). Reactive oxygen species burst induced by aluminum stress triggers mitochondria-dependent programmed cell death in peanut root tip cells. *Plant Physiology and Biochemistry*, 82, 76-84.

Husen, A., & Siddiqi, K. S. (2014). Phytosynthesis of nanoparticles: Concept, controversy and application. *Nanoscale Research Letters*, 9, 229-252.

Jiang, H. S., Qiu, X. N., Li, G. B., Li, W., & Yin, L. Y. (2014). Silver nanoparticles induced accumulation of reactive oxygen species and alteration of antioxidant systems in the aquatic plant *Spirodela polyrhiza*. *Environmental Toxicology & Chemistry*, 33(6), 1398-1405.

Kaiser, B. N., Gridley, K. L., Brady, J. N., Phillips, T., & Tyerman, S. D. (2005). The Role of Molybdenum in Agricultural Plant Production. *Annals of Botany*, 96(5), 745-754.

Khodakovskaya, M. V., de Silva, K., Biris, A. S., Dervishi, E., & Villagarcia, H. (2012). Carbon nanotubes induce growth enhancement of tobacco cells. *ACS Nano*, 6(3), 2128-2135.

Kim, S., Lee, S., & Lee, I. (2012). Alteration of Phytotoxicity and Oxidant Stress Potential by Metal Oxide Nanoparticles in *Cucumis sativus*. *Water, Air, & Soil Pollution*, 223(5), 2799-2806.

Kirschbaum, M. (2011). Does enhanced photosynthesis enhance growth? Lessons learned from CO_2 enrichment studies. *Plant Physiology*, 155, 117-124.

Kote, C., Kole, P., Randunu, K. M., Choudhary, P., Podila, R., Ke, P., & Marcus, R. K. (2013). Nanobiotechnology can boost crop production and quality: First evidence from increased plant biomass, fruit yield and phytomedicine content in bitter melon (*Momordica charantia*). *BMC Biotechnology*, 13, 37-46.

Kong, B., Seog, J. H., Graham, L. M., & Lee, S. B. (2011). Experimental considerations on the cytotoxicity of nanoparticles. *Nanomedicine*, 6(5), 929-941.

Koo, Y., Wang, J., Zhang, Q., Zhu, H., Chehab, E. W., Colvin, V. L., & Braam, J. (2015). Fluorescence Reports Intact Quantum Dot Uptake into Roots and Translocation to Leaves of *Arabidopsis thaliana* and Subsequent Ingestion by Insect Herbivores. *Environmental Science & Technology*, 49, 626−632.

Krishnaraj, C., Jagan, E. G., Ramachandran, R., Abirami, S. M., Mohan, N., & Kalaichelvan, P. T. (2012). Effect of biologically synthesized silver nanoparticles on *Bacopa monnieri* (*Linn*.) *Wettst*. Plant growth metabolism. *Process Biochemistry*, 47(4), 51-658.

Kroll, A., Pillukat, M.H., Hahn, D. & Schnekenburger, J. (2009). Current *in vitro* methods in nanoparticle risk assessment : Limitations and challenges. *European Journal of Pharmaceutics and Biopharmaceutics*, 72 (2), 370–377.

Lei, Z., Mingyu, S., Chao, L., Liang, C., Hao, H., Xiao, W., & Fashui, H. (2007). Effects of nanoanatase TiO_2 on photosynthesis of spinach chloroplasts under different light illumination. *Biological Trace Element Research*, 119, 68-76.

Li, Y., Song, Y., & Shi, G. (2009). Response of antioxidant activity to excess copper in two cultivars of *Brassica campestris* ssp. *chinensis Makino*. *Acta Physiologiae Plantarum*, 31(1), 155-162.

Li, W., Zheng, Y., Zhang, H., Liu, Z., Su, W., Chen, S., & Lei, B. (2016). Phytotoxicity, uptake, and translocation of fluorescent carbon dots in mung bean plants. *ACS Applied Materials & Interfaces*, 8, 19939-19945.

Li, Z. J., Li, X. B., Wang , J. J., Yu, S., Li, C. B., Tung, C. H., & Wu, L. Z. (2013). A robust "artificial catalyst" in situ formed from CdTe QDs and inorganic cobalt salts for photocatalytic hydrogen evolution. *Energy & Environmental Sciences*, 6(2), 465-469.

Lin, C., Fugetsu, B., Su, Y., & Watari, F. (2009). Studies on toxicity of multi-walled carbon nanotubes on *Arabidopsis* T87 suspension cells. *Journal of Hazardous Materials*, 170(2-3), 578-583.

Lin, S., Reppert, J., Hu, Q., Hudson, J. S., Reid, M. L., Ratnikova, T. A., & Ke, P. C. (2009). Uptake, translocation, and transmission of carbon nanomaterials in rice plants. *Small*, 5(10), 1128-1132.

Liu, Q., Chen, B., Wang, Q., Shi, X., Xiao, Z., Lin, J., & Fang, X. (2009). Carbon nanotubes as molecular transporters for walled plant cells. *Nano Letters*, 9, 1007-1010.

Liu, R., Zhang, H., & Lal, R. (2016). Effects of Stabilized Nanoparticles of Copper, Zinc, Manganese, and Iron Oxides in Low Concentrations on Lettuce (*Lactuca sativa*) Seed Germination: Nanotoxicants or Nanonutrients?, *Water, Air, & Soil Pollution*, 227(42).

Lopez-Moreno, M. L., de la Rosa, G., Hernandez-Viezcas, J. A., Castillo-Michel, H., Botez, C. E., Peralta-Videa, J. R., & Gardea-Torresdey, J. L. (2010). Evidence of the differential biotransformation and genotoxicity of ZnO and CeO_2 nanoparticles on soybean (*Glycine max*) plants. *Environmental Science & Technology*, 44(19), 7315-7320.

Lovrić, J., Bazzi, H. S., Cuie, Y., Fortin, G. R., Winnik, F. M., & Maysinger, D. (2005). Differences in subcellular distribution and toxicity of green and red emitting CdTe quantum dots. *Journal of Molecular Medicine*, 83(5), 377-385.

Lu, C. M., Zhang, C. Y., Wen, J. Q., Wu, G. R., & Tao, M. X. (2002). Research on the effect of nanometer materials on germination and growth enhancement of *Glycine max* and its mechanism. *Soybean Science*, 21, 68-172.

Ma, C., Chhikara, S., Xing, B., Musante, C., White, J. C., & Dhankher, O. P. (2013). Physiological and molecular response of *Arabidopsis thaliana* (L.) to nanoparticle cerium and indium oxide exposure. *ACS Sustainable Chemistry & Engineering*, 1(7), 768-778.

Mahajan, P., Dhoke, S. K., & Khanna, A. S. (2011). Effect of nano-ZnO particle suspension on growth of mung (*Vigna radiata*) and gram (*Cicer arietinum*) seedlings using plant agar method. *Journal of Nanotechnology*, 1–7.

Mancini, M. C., Kairdolf, B. A., Smith, A. M., & Nie, S. (2008). Oxidative quenching and degradation of polymer-encapsulated quantum dots: New insights into the long-term fate and toxicity of nanocrystals *in vivo*. *Journal of the American Chemical Society*, 130(33), 10836-10369.

Mattiello, A., Pošćić, F., Fellet, G., Zavalloni, C., Fontana, M., Piani, B., & Marchiol, L. (2016). Engineered Nanomaterials and Crops: Physiology and Growth of Barley as Affected by Nanoscale Cerium Oxide. *Journal of Agricultural Engineering*, 11(3).

Miralles, P., Church, T. L., & Harris, A. T. (2012). Toxicity, uptake, and translocation of engineered nanomaterials in vascular plants. *Environmental Science & Technology*, 46, 9224-9239.

Monreal, C. M., DeRosa, M., Mallubhotla, S. C., Bindraban, P. S., & Dimkpa, C. (2015). The Application of Nanotechnology for Micronutrients in Soil-Plant Systems. Washington, D.C: VFRC Report 2015/3.

Montalvo, D., McLaughlin, M. J., & Degryse, F. (2015). Efficacy of Hydroxyapatite Nanoparticles as Phosphorus Fertilizer in Andisols and Oxisols. *Soil Science Society of America*, 79(2), 551-558.

Mukherjee, A., Sun, Y., Morelis, E., Tamez, C., Bandyopadhyay, S., Niu, G., & Gardea-Torresdey, J. L. (2016). Differential Toxicity of Bare and Hybrid ZnO Nanoparticles in Green Pea (*Pisum sativum* L.): A Life Cycle Study. *Frontiers in Plant Science*, 6, 1-13.

Nair, R., Varghese, S. H., Nair, B. G., Maekawa, T., Yoshida, Y., & Kumar, D. S. (2010). Nanoparticulate material delivery to plants. *Plant Science*, 179(3), 154-163.

Namdari, P., Negahdari, B., & Eatemadi, A. (2017). Synthesis, properties and biomedical applications of carbon-based quantum dots: An updated review. *Biomedicine & Pharmacotherapy*, 87, 209-222.

Navarro, D. A., Banerjee, S., Watson, D. F., & Aga, D. S. (2011). Differences in Soil Mobility and Degradability between Water-Dispersible CdSe and CdSe/ZnS Quantum Dots. *Environmental Science & Technology*, 45, 6343–6349.

Nel, A., Xia, T., Madler, L., & Li, N. (2006). Toxic potential of materials at the nanolevel. *Science*, 311, 622-627.

Nikalje, A.P. (2015). Nanotechnology and its applications in medicine. *Medicinal chemistry*, 5 (2), 81-89.

Nussaume, L., Kanno, S., Javot, H., Marin, E., Pochon, N., Ayadi, A., & Thibaud, M. C. (2011). Phosphate import in plants: focus on the PHT1 transporters. *Frontiers in Plant Science*, 2, 1-12.

Onelli, E., Prescianotto-Baschong, C., Caccianiga, M., & Moscatelli, A. (2008). Clathrin dependent and independent endocytic pathways in tobacco protoplasts revealed by labelling with charged nanogold. *Journal of Experimental Botany*, 59(11), 3051-3068.

Pariona, N., Martinez, A. I., Hdz-Garcı´a, H. M., Cruz, L. A., & Hernandez-Valdes, A. (2016). Effects of hematite and ferrihydrite nanoparticles on germination and growth of maize seedlings. *Saudi Journal of Biological Sciences*, 1-8.

Peng, X., Yu, W. W., Qu, L., & Guo, W. (2003). Experimental Determination of the Extinction Coefficient of CdTe, CdSe, and CdS Nanocrystals. *Chemistry of Materials*, 15(14), 2854-2860.

Prasad, R., Pandey, R., & Barman, I. (2016). Engineering tailored nanoparticles with microbes: quo vadis?, *Nanomedicine and Nanobiotechnology*, 8(2), 313-330.

Prasad, T., Sudhakar, P., Sreenivasulu, Y., Latha, P., Munaswamy, V., Reddy, K. R., & Pradeep, T. (2012). Effect of nanoscale zinc oxide particles on the germination, growth and yield of peanut. *Journal of Plant Nutrition*, 35(6), 905-927.

Priyanka, N., & Venkatachalam, P. (2016). Biofabricated zinc oxide nanoparticles coated with phycomolecules as novel micronutrient catalysts for stimulating plant growth of cotton. Advances in Natural Sciences: *Nanoscience and Nanotechnology*, 7, 1-11.

Purvis, E. R. (1955). Review of the role of Molybdenum in soils and plants. Journal of *Agricultural & Food Chemistry*, 3(8), 665-665.

Qi, M., Liu, Y., & Li, T. (2013). Nano-TiO_2 improve the photosynthesis of tomato leaves under mild heat stress. *Biological Trace Element Research*, 156(1-3), 323-328.

Qian, H., Peng, X., Han, X., Ren, J., Sun, L., & Fu, Z. (2013). Comparison of the toxicity of silver nanoparticles and silver ions on the growth of terrestrial plant model *Arabidopsis thaliana*. *Journal of Environmental Sciences*, 25, 1947-1956.

Quan, L. J., Zhang, B., Shi, W. W., & Li, H. Y. (2008). Hydrogen peroxide in plants: a versatile molecule of the reactive oxygen species network. *Journal of Integrative Plant Biology*, 50(1), 2-18.

Raliya, R., & Tarafdar, J. C. (2013). ZnO nanoparticle biosynthesis and its effect on phosphorous-mobilizing enzyme secretion and gum contents in cluster bean (*Cyamopsis tetragonoloba* L.). *Agricultural Research*, 2, 48-57.

Ramesh, M., Palanisamy, K., Babu, K., & Sharma, N. K. (2014). Effects of bulk & nano-titanium dioxide and zinc oxide on physio-morphological changes in *Triticum aestivum* Linn. *Journal of Global Biosciences*, 3, 415-422.

Raskar, S. V., & Laware, S. L. (2014). Effect of zinc oxide nanoparticles on cytology and seed germination in onion. *International Journal of Current Microbiology and Applied Sciences*, 3, 467-473.

Riahi-Madvar, A., Rezaee, F., & Jalali, V. (2012). Effects of alumina nanoparticles on morphological properties and antioxidant system of *Triticum aestivum*. *Iranian Journal of Plant Physiology*, 3(1), 595-603.

Rico, C. M., Morales, M. I., Barrios, A. C., McCreary, R., Hong, J., Lee, W. Y., & Gardea-Torresdey, J. L. (2013). Effect of Cerium Oxide Nanoparticles on the Quality of Rice (*Oryza sativa* L.) Grains. Journal of Agricultural & Food Chemistry, 61, 1278-11285.

Russo, D., Valentao, P., Andrade, P. B., Fernandez, E. C., & Milella, L. (2015). Evaluation of antioxidant, antidiabetic and anticholinesterase activities of *Smallanthus sonchifolius* Landraces and correlation with their phytochemical profiles. *International Journal of Molecular Sciences, 16*, 17696-17718.

Salama, H. (2012). Effects of silver nanoparticles in some crop plants, common bean (*Phaseolus vulgaris* L.) and corn (*Zea mays* L.). *International Research Journal of Biotechnology*, 3(10), 190-197.

Sanevas, N., Sunohara, Y., & Matsumoto, H. (2007). Characterization of reactive oxygen species involved oxidative damage in *Hapalosiphon* species crude extract-treated wheat and onion roots. *Weed Biology and Management*, 7, 172-177.

Santos, A. R., Miguel, A. S., Macovei, A., Maycock, C., Balestrazzi, A., Oliva, A., & Fevereiro, P. (2013). CdSe/ZnS Quantum Dots trigger DNA repair and antioxidant enzyme systems in *Medicago sativa* cells in suspension culture. *BMC Biotechnology*, 13(111), 1-11.

Santos, A. R., Miguel, A. S., Tomaz, L., Malhó, R., Maycock, C., Vaz Patto, M. C., & Oliva, A. (2010). The impact of CdSe/ZnS Quantum Dots in cells of *Medicago sativa* in suspension culture. *Journal of Nanobiotechnology*, 8(24), 1-14.

Sedghi, M., Hadi, M., & Toluie, S. G. (2013). Effect of nano zinc oxide on the germination of soybean seeds under drought stress. Annals of West University of Timisoara, Series of Biology XVI, 2, 73-78.

Sharma, P., Bhatt, D., Zaidi, M. G., Saradhi, P. P., Khanna, P. K., & Arora, S. (2012). Silver nanoparticle-mediated enhancement in growth and antioxidant status of *Brassica juncea*. *Applied Biochemistry and Biotechnology*, 167, 2225-2233.

Sharma, P., Jha, A. B., Dubey, R. S., & Pessarakli, M. (2012). Reactive Oxygen Species, Oxidative Damage, and Antioxidative Defense Mechanism in Plants under Stressful Conditions. *Hindawi Journal of Botany*, 1-26.

Shen, C. X., Zhang, Q. F., Li, J., Bi, F. C., & Yao, N. (2010). Induction of programmed cell death in Arabidopsis and rice by single-wall carbon nanotubes. *American Journal of Botany*, 97(10), 1602-1609.

Shen, M., Jia, W., You, Y., Hu, Y., Li, F., Tian, S., & Han, D. (2013). Luminescent properties of CdTe quantum dots synthesized using 3-mercaptopropionic acid reduction of tellurium dioxide directly. *Nanoscale Research Letters*, 8(253), 1-6.

Shereema, R. M., Sankar, V., Raghu, K. G., Talasila, P. R., & Shankar, S. S. (2015). One step green synthesis of carbon quantum dots and its application towards the bioelectricoanalytical and biolabelling studies. *Electrochimica Acta*, 182, 588-595.

Siddiqui, M. H., Al-Whaibi, M. H., Faisal, M., & Al Sahli, A. (2014). Nano-silicon dioxide mitigates the adverse effects of salt stress on *Cucurbita pepo* L. *Environmental Toxicology and Chemistry*, 33(11), 2429-2437.

Siddiqui, M. H., Al-Whaibi, M. H., Firoz, M., & Al-Khaishany, M. Y. (2015). Role of Nanoparticles in Plants. In Nanotechnology and Plant Sciences (pp. 19-35). Springer International Publishing Switzerland.

Singh, S., Garg, S., Chahal, J., Raheja, K., Singh, D., & Singla, M. L. (2013). Luminescent behaviour of cadmium sulfide quantum dots for gallic acid estimation. *Nanotechnology*, 24, 1-8.

Sumanta, N., Haque, C. I., Nishika, J., & Suprakash, R. (2014). Spectrophotometric Analysis of Chlorophylls and Carotenoids from Commonly Grown Fern Species by Using Various Extracting Solvents. *Research Journal of Chemical Sciences*, 4(9), 63-69.

Thambiraj, S., & Shankaran, D. R. (2016). Green synthesis of highly fluorescent carbon quantum dots from sugarcane bagasse pulp. *Applied Surface Science*, 390, 435-443.

Tripathi, D. K., Shweta, Singh, S., Singh, S., Pandey, R., Singh, P. V., & Chauhan, D. K. (2017). An overview on manufactured nanoparticles in plants: Uptake, translocation, accumulation and phytotoxicity. *Plant Physiology and Biochemistry*, 110, 2-12.

Tripathi, D. K., Singh, V. P., Swati, S., Prasad, S. M., Chauhan, D. K., & Dubey, N. K. (2016). Effect of silicon and silicon nanoparticle (SiNp) on seedlings of maize cultivar and hybrid differing in arsenate tolerance. *Frontiers in Environmental Science*, 4(46), 1-14.

Trujillo-Reyes, J., Majumdar, S., Botez, C. E., Peralta-Videa, J. R., & Gardea-Torresdey, J. L. (2014). Exposure studies of core–shell Fe/Fe3O4 and Cu/CuO NPs to lettuce (*Lactuca sativa*) plants: are they a potential physiological and nutritional hazard?, *Journal of Hazardous Materials*, 267, 255-263.

Tsurushima, T., Minami, Y., Miyagawa, H., Nakayashiki, H., Tosa, Y., & Mayama, S. (2010). Induction of chlorosis, ROS generation and cell death by a toxin isolated from *Pyricularia oryzae*. *Bioscience, Biotechnology, and Biochemistry*, 74(11), 2220-2225.

Vance, C. P., Uhde-Stone, C., & Allan, D. L. (2003). Phosphorus acquisition and use: critical adaptations by plants for securing a nonrenewable resource. *New Phytologist*, 157(3), 423-447.

Vaneckova, T., Sturikova, H., Milosavljevic, V., Kopel, P., Krystofova, O., Vaculovicova, M., & Adam, V. (2016). In vivo fluorescence visualization of quantum dot nanopartices in plants. *MendelNet*, 1026-1030.

Velikova, V., Yordanov, I., & Edreva, A. (2000). Oxidative Stress and Some Antioxidant Systems in Acid Rain Treated Bean Plants: Protective Role of Exogenous Polyamines. *Plant Science*, 151, 59-66.

Veronica, N., Tulasi, G., Thatikunta, R., & Reddy, N. S. (2005). Nano fertilizers and their roles in sustainable agriculture. *International Journal of Environmental Science and Technology*, 1(1), 1-3.

Wang, A., Zheng, Y., & Peng, F. (2014). Thickness-controllable silica coating of CdTe QDs by reverse microemulsion method for the application in the growth of rice. *Journal of Spectroscopy*. doi:http://dx.doi.org/10.1155/2014/169245.

Wang, H. F., Zhong, X. H., Shi, W. Y., & Guo, B. (2011). Study of malondialdehyde (MDA) content, superoxide dismutase (SOD) and glutathione peroxidase (GSH-Px) activities in chickens infected with avian infectious bronchitis virus. *African Journal of Biotechnology*, 10, 9213-9217.

Wang, Y., & Hu, A. (2014). Carbon quantum dots: synthesis, properties and applications. *Journal of Materials Chemistry C*, 2, 6921-6939.

Wang, Z., Xie, X., Zhao, J., Liu, X., Feng, W., White, J. C., & Xing, B. (2012). Xylem-and phloem-based transport of CuO nanoparticles in maize (*Zea mays* L.). *Environmental Science & Technology*, 46(8), 4434-4441.

Wissuwa, M., Ismail, A. M., & Yanagihara, S. (2006). Effects of zinc deficiency on rice growth and genetic factors contributing to tolerance. *Plant Physiology*, 142(2), 731-741.

Yan, C., Tang, F., Li, L., Li, H., Huang, X., Chen, D., & Ren, J. (2010). Synthesis of Aqueous CdTe/CdS/ZnS Core/shell/shell Quantum Dots by a Chemical Aerosol Flow Method. *Nanoscale Research Letters*, 5, 89-194.

Yang, F., Hong, F., You, W., Liu, C., Gao, F., Wu, C., & Yang, P. (2006). Influence of nano-anatase TiO_2 on the nitrogen metabolism of growing spinach. *Biological Trace Element Research*, 110(2), 179-190.

Yang, J., Cao, W., & Rui, Y. (2017). Interactions between nanoparticles and plants: phytotoxicity and defence mechanisms. *Journal of Plant Interactions*, 12(1), 158-169.

Yu, G., Tan, Y., He, X., Qin, Y., & Liang, J. (2014). CLAVATA3 Dodecapeptide Modified CdTe Nanoparticles: A Biocompatible Quantum Dot Probe for *In Vivo* Labelling of Plant Stem Cells. *PLOS ONE*, 9(2), 1-9.

Yu, Y., Zhang, K., Li, Z., & Sun, S. (2012). Synthesis and luminescence characteristics of DHLA-capped PbSe quantum dots with biocompatibility. *Optical Materials*, 34, 793-798.

Zhang, F., Wang, Y., Lou, Z., & Dong, J. (2007). Effect of heavy metal stress on antioxidative enzymes and lipid peroxidation in leaves and roots of two mangrove plant seedlings (*Kandelia candel* and *Bruguiera gymnorrhiza*). *Chemosphere*, 67, 44–50.

Zhang, P., Ma, Y., & Zhang, Z. (2015). Interactions between engineered nanoparticles and plants: phytotoxicity, uptake, translocation, and biotransformation. In Nanotechnology and Plant Sciences (pp. 77-99). Springer International Publishing.

Zhao, L., Peng, B., Hernandez-Viezcas, J. A., Rico, C., Sun, Y., Peralta-Videa, J. R., & Varela-Ramirez, A. (2012). Stress response and tolerance of *Zea mays* to CeO_2 nanoparticles: cross talk among H_2O_2, heat shock protein, and lipid peroxidation. *ACS Nano*, 6, 9615–9622.

Zhao, L., Peralta-Videa, J. R., Peng, B., Bandyopadhyay, S., Corral-Diaz, B., Osuna-Avila, P., & Gardea-Torresdey, J. L. (2014). Alginate modifies the physiological impact of CeO_2 nanoparticles in corn seedlings cultivated in soil. *Journal of Environmental Science*, 26, 382-389.

Zhao, L., Peralta-Videa, J. R., Rico, C. M., Hernandez-Viezcas, J. A., Sun, Y., Niu, G., & Gardea-Torresdey, J. L. (2014). CeO_2 and ZnO nanoparticles change the nutritional qualities of cucumber (*Cucumis sativus*). *Journal of Agricultural & Food Chemistry*, 62(13), 2752-2759.

Zhao, L., Peralta-Videa, J. R., Varela-Ramirez, A., Castillo-Michel, H., Li, C., Zhang, J., & Gardea-Torresdey, J. L. (2012). Effect of surface coating and organic matter on the uptake of CeO_2–NPs by corn plants grown in soil: Insight into the uptake mechanism. *Journal of Hazardous Materials*, 131-138.

Zhao, L., Sun, Y., Hernandez-Viezcas, J. A., Servin, A. D., Hong, J., Niu, G., & Gardea-Torresdey, J. L. (2014). Influence of CeO_2 and ZnO nanoparticles on cucumber physiological markers and bioaccumulation of Ce and Zn: a life cycle study. *Journal of Agricultural and Food Chemistry*, 61, 11945–11951.

Zheng, L., Hong, F., Lu, S., & Liu, C. (2005). Effect of nano-TiO_2 on strength of naturally aged seeds and growth of spinach. *Biological Trace Element Research*, 104(1), 83-91.

Zhu, H., Han, J., Xiao, J. Q., & Jin, Y. (2008). Uptake, translocation, and accumulation of manufactured iron oxide nanoparticles by pumpkin plants. *Journal of Environmental Monitoring*, 10, 713-717.

Zuverza-Mena, N., Armendariz, R., Peralta-Videa, J. R., & Gardea-Torresdey, J. L. (2016). Effects of Silver Nanoparticles on Radish Sprouts: Root Growth Reduction and Modifications in the Nutrition Value. *Frontiers in Plant Science*, 7, 1-11.

Supplementary Data

Supplementary Table 1: Elemental concentrations (µg. g^{-1}) in the leaves of *P. vulgaris.*

		Control	MPA-CdTe QDs	Carbon QDs
Macronutrients	**K**	630.55 ± 40.08 ^{b}	771.61 ± 36.77 ^{a}	655.87 ± 29.96 ^{b}
	Ca	364.41 ± 7.51 ^{c}	432.89 ± 68.50 ^{b}	508.36 ± 11.11 ^{a}
	Mg	146.20 ± 2.79 ^{a}	81.53 ± 5.42 ^{c}	119.95 ± 4.53 ^{b}
	P	51.54 ± 4.71 ^{a}	48.51 ± 2.02 ^{b}	45.07 ± 2.79 ^{b}
Micronutrients	**Cu**	25.48 ± 1.49 ^{a}	20.01 ± 0.93 ^{b}	14.60 ± 0.79 ^{c}
	Zn	1.76 ± 0.29 ^{c}	2.41 ± 0.25 ^{a}	1.50 ± 0.17 ^{b}
	Mo	5.76 ± 0.97 ^{b}	3.93 ± 0.98 ^{c}	6.89 ± 1.13 ^{a}
	Mn	8.93 ± 0.42 ^{a}	3.45 ± 0.57 ^{c}	7.86 ± 0.67 ^{b}
	Fe	6.67 ± 0.45 ^{b}	5.35 ± 0.19 ^{c}	7.21 ± 0.25 ^{a}

Different letters indicate significant difference between means at P < 0.05 (DMRT) per row. Values are means ± SD (n=3).

Supplementary Table 2: Elemental concentrations (µg. g^{-1}) in the roots of *P. vulgaris*.

		Control	MPA-CdTe QDs	Carbon QDs
Macronutrients	**K**	480.35 ± 5.35 ^{c}	814.39 ± 39.17 ^{a}	672.49 ± 66.47 ^{b}
	Ca	471.80 ± 38.80 ^{b}	588.80 ± 61.01 ^{a}	388.87 ± 13.89 ^{c}
	Mg	93.33 ± 2.80 ^{c}	137.28 ± 12.50 ^{a}	120.03 ± 6.70 ^{a}
	P	47.56 ± 2.22 ^{b}	57.60 ± 4.62 ^{a}	55.63 ± 5.81 ^{a}
Micronutrients	**Cu**	22.60 ± 0.56 ^{b}	25.92 ± 2.33 ^{a}	28.33 ± 3.04 ^{a}
	Zn	10.35 ± 0.89 ^{a}	10.79 ± 1.58 ^{a}	12.32 ± 1.13 ^{a}
	Mo	4.68 ± 0.67 ^{a}	5.69 ± 0.66 ^{a}	6.65 ± 1.48 ^{a}
	Mn	20.69 ± 1.11 ^{a}	23.26 ± 2.50 ^{a}	25.36 ± 1.98 ^{a}
	Fe	25.11 ± 0.85 ^{b}	34.47 ± 4.84 ^{a}	27.48 ± 3.18 ^{a}

Different letters indicate significant difference between means at P < 0.05 (DMRT) per row. Values are means ± SD (n=3).

Supplementary Table 3: Elemental concentrations (µg. g^{-1}) in the leaves of *G. max*.

		Control	MPA-CdTe QDs	Carbon QDs
Macronutrients	**K**	767.07 ± 1.91 ^{b}	757.72 ± 40.71 ^{c}	961.37 ± 18.55 ^{a}
	Ca	245.05 ± 96.80 ^{c}	759.95 ± 23.45 ^{b}	779.70 ± 83.76 ^{a}
	Mg	115.61 ± 5.86 ^{c}	147.76 ± 0.57 ^{b}	195.28 ± 16.02 ^{a}
	P	74.68 ± 1.91 ^{b}	68.92 ± 3.32 ^{c}	94.87 ± 1.23 ^{a}
Micronutrients	**Cu**	38.10 ± 3.06 ^{a}	35.68 ± 3.51 ^{a}	37.28 ± 5.67 ^{b}
	Zn	3.37 ± 0.05 ^{c}	3.96 ± 0.47 ^{b}	6.20 ± 0.58 ^{a}
	Mo	0.63 ± 0.06 ^{b}	1.53 ± 0.57 ^{a}	1.77 ± 0.59 ^{a}
	Mn	6.66 ± 2.37 ^{c}	11.42 ± 0.89 ^{b}	13.93 ± 0.81 ^{a}
	Fe	10.10 ± 1.64 ^{b}	9.74 ± 0.70 ^{c}	14.17 ± 0.27 ^{a}

Different letters indicate significant difference between means at P < 0.05 (DMRT) per row. Values are means ± SD (n=3).

Supplementary Table 4: Elemental concentrations (µg. g^{-1}) in the roots of *G. max*.

		Control	MPA-CdTe QDs	Carbon QDs
Macronutrients	**K**	1085.07 ± 17.18 [b]	1421.60 ± 117.53 [a]	1375.49 ± 120.20 [a]
	Ca	639.61 ± 38.09 [c]	1252.26 ± 0.60 [a]	766.87 ± 7.68 [b]
	Mg	157.58 ± 6.86 [b]	230.32 ± 30.54 [a]	127.26 ± 3.51 [c]
	P	113.69 ± 9.92 [b]	137.09 ± 10.55 [a]	137.63 ± 11.59 [a]
Micronutrients	**Cu**	53.63 ± 1.85 [b]	62.50 ± 4.03 [a]	49.90 ± 3.50 [b]
	Zn	3.10 ± 0.22 [b]	4.80 ± 0.07 [a]	3.52 ± 0.05 [c]
	Mo	1.88 ± 0.01 [c]	2.08 ± 0.79 [b]	2.48 ± 0.04 [a]
	Mn	22.37 ± 0.99 [b]	33.63 ± 5.11 [a]	21.76 ± 1.80 [b]
	Fe	39.90 ± 0.12 [c]	66.03 ± 7.41 [b]	97.90 ± 3.87 [a]

Different letters indicate significant difference between means at P < 0.05 (DMRT) per row. Values are means ± SD (n=3).

Supplementary Table 5: Translocation factor of macro and micronutrients in *P. vulgaris*.

		Control	MPA-CdTe QDs	Carbon QDs
Macronutrients	**K**	1.31 ± 0.49 [a]	0.95 ± 0.94 [b]	0.98 ± 0.45 [b]
	Ca	0.77 ± 0.19 [a]	0.74 ± 0.12 [a]	1.31 ± 0.79 [a]
	Mg	1.57 ± 0.99 [a]	0.59 ± 0.43 [b]	0.99 ± 0.68 [b]
	P	1.08 ± 0.12 [a]	0.84 ± 0.44 [b]	0.81 ± 0.48 [b]
Micronutrients	**Cu**	1.13 ± 0.66 [a]	0.77 ± 0.4 [b]	0.52 ± 0.26 [b]
	Zn	0.17 ± 0.33 [a]	0.22 ± 0.16 [a]	0.12 ± 0.15 [a]
	Mo	1.23 ± 0.45 [a]	0.69 ± 1.48 [a]	1.04 ± 0.76 [b]
	Mn	0.43 ± 0.38 [a]	0.15 ± 0.23 [b]	0.31 ± 0.34 [a]
	Fe	0.27 ± 0.53 [a]	0.16 ± 0.04 [b]	0.26 ± 0.08 [a]

Different letters indicate significant difference between means at P < 0.05 (DMRT) per row. Values are means ± SD (n=3).

Supplementary Table 6: Translocation factor of macro and micronutrients in *G. max*.

		Control	MPA-CdTe QDs	Carbon QDs
Macronutrients	**K**	0.71 ± 0.11 [a]	0.53 ± 0.35 [a]	0.7 ± 0.15 [a]
	Ca	0.38 ± 0.54 [a]	0.61 ± 0.08 [b]	1.02 ± 0.9 [a]
	Mg	0.73 ± 0.85 [a]	0.64 ± 0.02 [b]	1.53 ± 0.56 [a]
	P	0.66 ± 0.19 [a]	0.5 ± 0.31 [b]	0.69 ± 0.11 [a]
Micronutrients	**Cu**	0.71 ± 0.65 [a]	0.57 ± 0.87 [b]	0.75 ± 0.62 [a]
	Zn	1.09 ± 0.22 [b]	0.82 ± 0.71 [b]	1.76 ± 0.16 [a]
	Mo	0.33 ± 0.6 [b]	0.74 ± 0.72 [a]	0.72 ± 0.47 [a]
	Mn	0.3 ± 0.39 [a]	0.34 ± 0.17 [b]	0.64 ± 0.45 [a]
	Fe	0.25 ± 0.67 [a]	0.15 ± 0.09 [b]	0.14 ± 0.07 [b]

Different letters indicate significant difference between means at P < 0.05 (DMRT) per row. Values are means ± SD (n=3).